ACCELERATOR GROUP
European Physical Society

IPAC23

14th International Particle Accelerator Conference

IPAC '23

7 - 12 May 2023

VENICE, ITALY

IPAC23

Anne-Marie Valente-Feliciano

Superconducting RF Cavities for Particle Accelerators

Jefferson Lab

OUTLINE

- Introduction to RF Cavities
- Normal-conductors
- Superconductors
- Surface impedance
  - Two-fluid model and BCS theory
- Residual resistance
- Superheating field
- Field dependence of the surface resistance due to thermal feedback
- Design Considerations
- Example of SRF Cavities

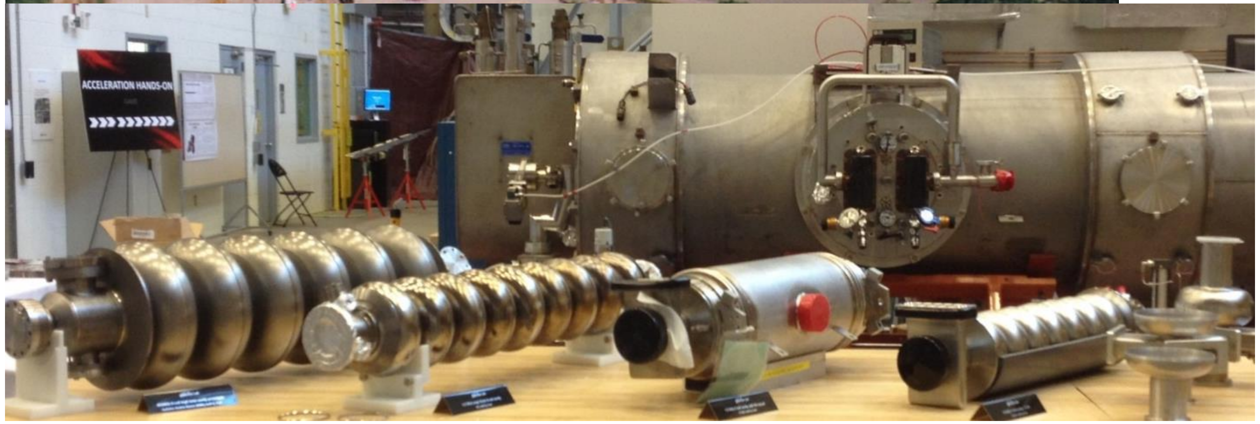

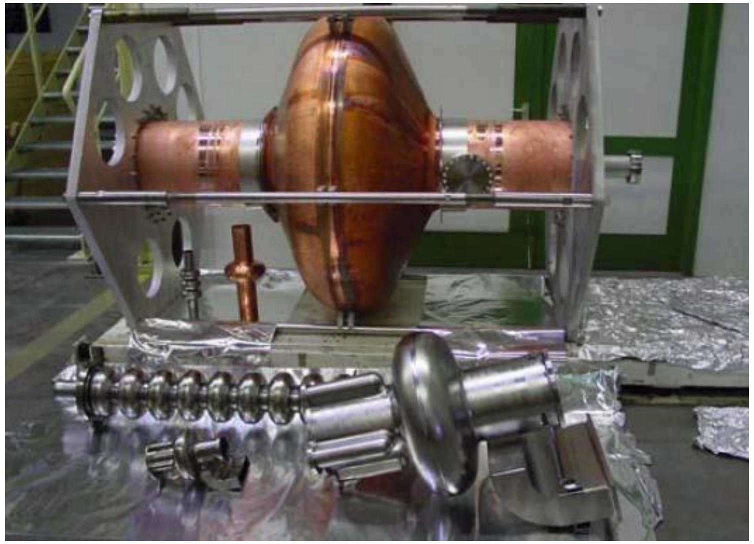

TECHNICAL MOTIVATION FOR SUPERCONDUCTING RF CAVITIES

The principle motivations for using superconducting RF cavities, are:

High duty cycle or cw operation.

SRF cavities allow the excitation of high electromagnetic fields at high duty cycle, or even cw, in such regimes that a copper cavity's electrical loss could melt the copper, even with robust water cooling.

SRF Cavities

Large variety, depending on:

- Type of accelerator
- Particle velocity
- Current and Duty factor
- Gradient
- Acceleration or deflecting mode

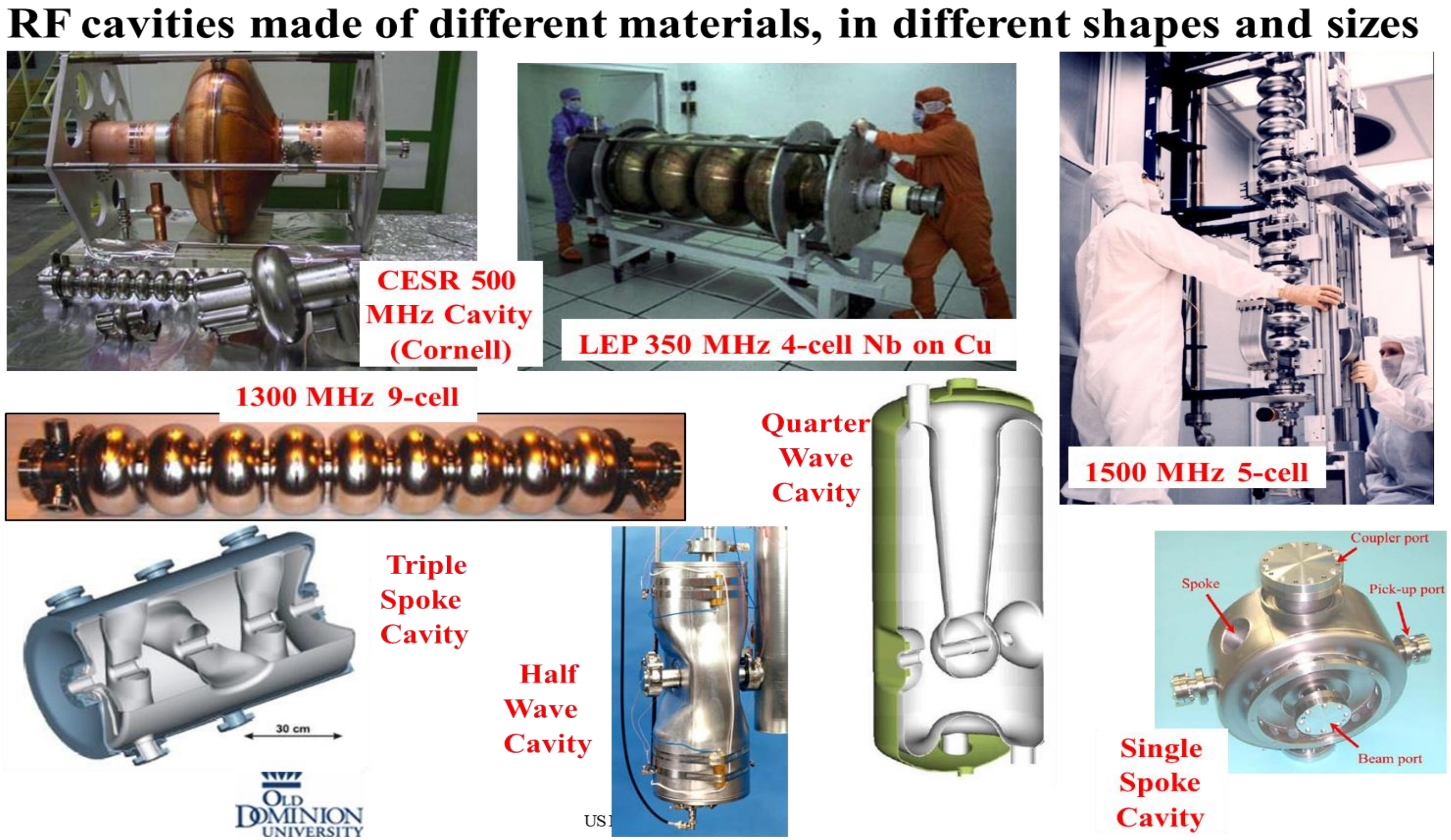

Modern SRF cavities cover wide range of particles beta (0.05..1), operating frequencies (0.072..4 GHz) and beam currents (1mA..100mA, CW & Pulsed)

RF Cavities

- Space enclosed by conducting walls that can sustain an infinite number of resonant electromagnetic modes

- Shape is selected so that a particular mode can efficiently transfer its energy to a charged particle

- An isolated mode can be modeled by an LRC circuit

- Lorentz force $\vec{F} = q(\vec{E} + \vec{v} \times \vec{B})$

- An accelerating cavity needs to provide an electric field (E) longitudinal with the velocity of the particle
- Magnetic fields (H) provide deflection but no acceleration

RF Cavities

- Devices that store e.m. energy and transfer it to a charged particle beam

enclosed by conducting walls that can sustain an infinite number of resonant electromagnetic modes

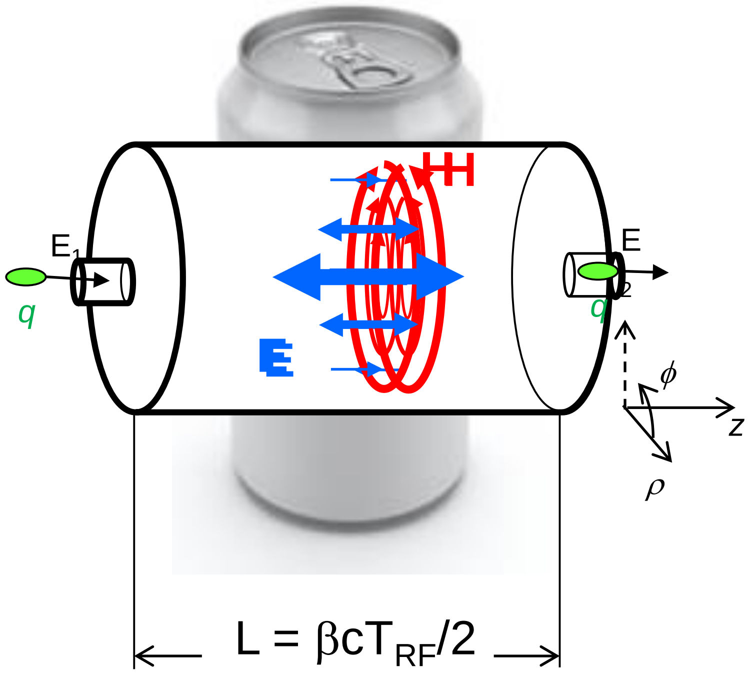

- E.m. field in the cavity is solution to the wave equation

$$\left(\nabla^2 - \frac{1}{c^2}\frac{\partial^2}{\partial t^2}\right)\begin{Bmatrix}\mathbf{E}\\ \mathbf{H}\end{Bmatrix} = 0 \qquad \hat{n}\times\mathbf{E} = 0, \quad \hat{n}\cdot\mathbf{H} = 0$$

- Solutions are two family of modes with different eigenfrequencies
  - **TE_{mnp} modes have only transverse electric fields**
  - **TM_{mnp} modes have only transverse magnetic fields (but longitudinal component for E)**

- Accelerating mode: TM_{010}

$$E_z = E_0 J_0\left(\frac{2.405\rho}{R}\right) e^{-i\omega t}$$

$$H_\phi = -i\frac{E_0}{\eta} J_1\left(\frac{2.405\rho}{R}\right) e^{-i\omega t}$$

$$\omega_{010} = \frac{2.405c}{R} \qquad \eta = \sqrt{\frac{\mu_0}{\epsilon_0}}$$

Example: 2 GHz cavity and speed of light e^- $\rightarrow$ L = 7.5 cm, R = 5.7 cm

Figures of merit (1)

Jefferson Lab

- *What is the energy gained by the particle?*
- Let's assume a relativistic e$^-$
- Integrate the E-field at the particle position as it traverses the cavity

$$V_c = \left| \int_0^d E_z(\rho = 0, z) e^{i\omega_0 z/c} dz \right| = \frac{2}{\pi} E_0 L$$

- We can define the **accelerating field** a $E_{acc} = \frac{V_c}{L} = \frac{2}{\pi} E_0$

Important for the cavity performance are the ratios of the **peak surface fields** to the E_{acc}.
Ideally, these should be small to limit losses and other troubles at high fields

$$E_p / E_{acc} = \frac{\pi}{2} = 1.6$$

$$H_p / E_{acc} = \frac{\pi}{2} \frac{J_1(1.84)}{\eta} = 2430 \frac{\mathrm{A/m}}{\mathrm{MV/m}} = 30.5 \frac{\mathrm{Oe}}{\mathrm{MV/m}}$$

Figures of merit (2)

- The **power dissipated** in the cavity wall due to Joule heating is given by:

$$P_c = \frac{1}{2}\mathrm{Re}\left\{\int_V \mathbf{J}\cdot\mathbf{E}\,dV\right\} = \frac{1}{2}R_s\int_S |H|^2 ds$$

- The **energy stored** in the cavity is given by: $U = \frac{1}{2}\mu_0 \int_V |\mathbf{H}|^2 dv$

- The cavity **quality factor** is defined as:

$$Q_0 = \frac{\omega_0 U}{P_c} = \frac{\omega_0\mu_0\int_V |\mathbf{H}|^2 dv}{R_S\int_S |\mathbf{H}|^2 ds} = \frac{\omega_0}{\Delta\omega}$$

= G

Geometry Factor

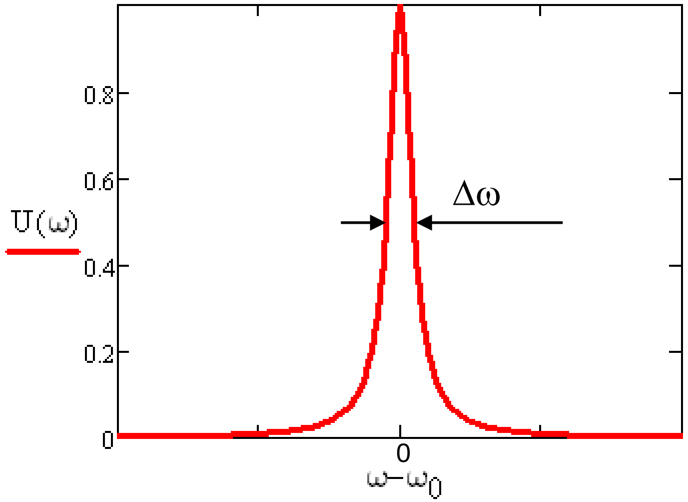

- Independent of size and material
- Depends only on shape of cavity and electromagnetic mode

very useful for comparing different cavity shapes.

SRF cavity performance – Q vs. E_{acc}

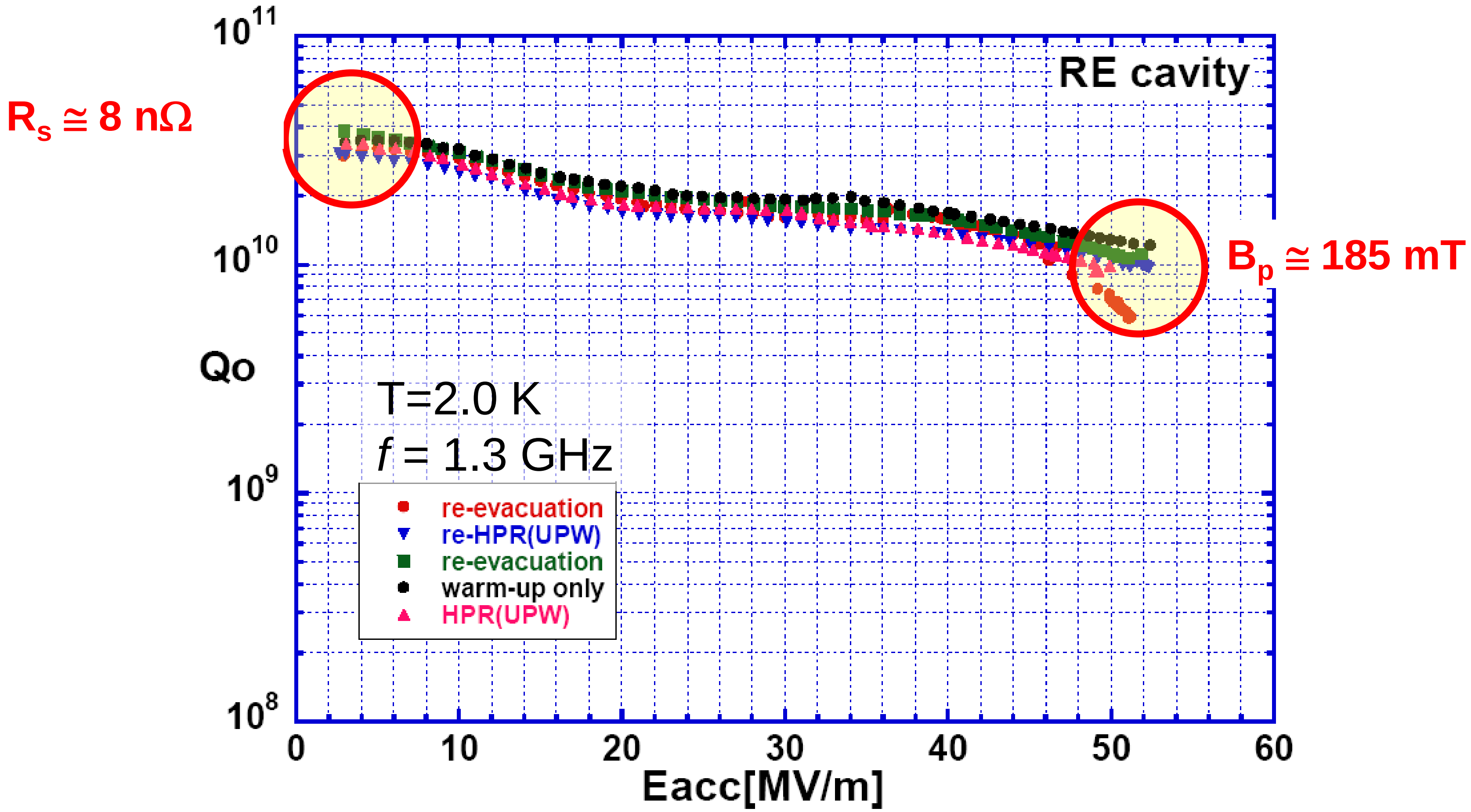

F. Furuta et al., Proc. EPAC'06, p. 750

Surface Impedance

- The electromagnetic response of a metal, whether normal or superconducting, is described by a complex surface impedance:

$$Z_s = \frac{|E_\parallel|}{\int_0^\infty J(x)dx} = \frac{E_\parallel}{H_\parallel} = R_s + iX_s$$

surface reactance

surface resistance

For a good conductor and $\omega <\sim 10^{16}$ Hz $\frac{\partial D}{\partial t} \approx 0 \rightarrow \nabla \times H = J$

- The impedance of vacuum is: $Z_0 = \left(\frac{\mu_0}{\varepsilon_0}\right)^{1/2} \simeq 377\Omega$

For accelerator applications, the rate of oscillation of the e.m. field falls in the radio-frequency (RF) range (3 kHz – 300 GHz)

Electrodynamics of normal conductors

Electrons in real metals show Ohmic loss

$$\nabla \cdot E = \frac{\rho}{\varepsilon_0} \qquad \nabla \times E = -\frac{\partial B}{\partial t}$$

$$\nabla \cdot B = 0 \qquad \nabla \times H = J + \frac{\partial D}{\partial t}$$

Maxwell's equations

+

$$D = \varepsilon_0 \varepsilon \ E$$

$$B = \mu_0 \mu \ H$$

$$J = f\ (E)$$

(linear and isotropic) material's equations

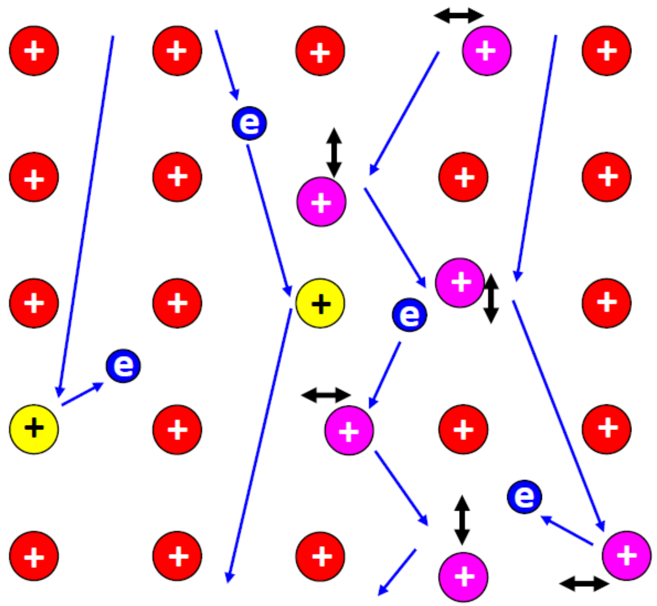

Imperfections causes local scattering

- From Drude's model ("nearly free electrons"), macroscopic phenomenology :

$$E = E_0 e^{i\omega t} \qquad \frac{\partial J}{\partial t} + \frac{J}{\tau} = \frac{ne^2}{m} E$$

$\tau = l/v_F \approx 10^{-14}$ s is the electrons' scattering time

$$J = \frac{ne^2}{m\tau} \frac{1}{(1 + i\omega\tau)} E = \sigma E$$

Ohm's law, <u>local</u> relation between *J* and *E*

$\omega\tau \ll 1$ at RF frequencies

Electrical conductivity σ

Surface impedance of normal conductors

- From previous slide you obtain:

$$\nabla^2 H = i\sigma\mu_0\mu\omega H$$

- Solution (semi-infinite slab):

$$H_y = H_0 e^{-x/\delta} e^{-ix/\delta}$$

$$E_z = -\frac{(1+i)}{\sigma\delta} H_y$$

skin depth:

$$\boxed{\delta = \sqrt{\frac{2}{\mu_0\mu\sigma\omega}}}$$

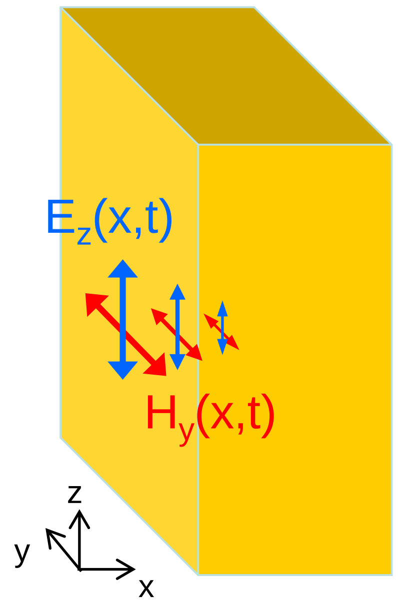

$$Z_s = \frac{|E_z(0)|}{H_y(0)} = \frac{1+i}{\sigma\delta}$$

$$\boxed{R_s = X_s = \frac{1}{\sigma\delta} = \sqrt{\frac{\mu_0\mu\omega}{2\sigma}}}$$

Example: Cu at 1.5 GHz, 300 K ($\sigma = 5.8\times10^7$ 1/Ωm, $\mu_0 = 1.26\times10^{-6}$ Vs/Am, $\mu = 1$)

$\Rightarrow$ δ = 1.7 μm, R_s = 10 mΩ

What happens at low temperature?

- $\sigma(T)$ increases, δ decreases ➡ The skin depth (the distance over which fields vary) can become less than the mean free path of the electrons (the distance they travel before being scattered)

➡ $J(x) \neq \sigma E(x)$

- Introduce a new relationship where *J* is related to *E* over a volume of the size of the mean free path (*l*)

$$\vec{J}(\vec{r},t) = \frac{3\sigma}{4\pi l}\int_V d\vec{r}' \, \frac{\vec{R}\left[\vec{R}\cdot\vec{E}(\vec{r}',t-\vec{R}/v_F)\right]}{R^4} e^{-R/l} \quad \text{with} \quad \vec{R} = \vec{r}' - \vec{r}$$

Effective conductivity $\quad \sigma_{eff} \approx \frac{\delta}{l}\sigma = \frac{\delta}{l}\frac{ne^2 l}{m v_F}$

$= \tau$

Contrary to the DC case higher purity (longer *l*) does not increase the conductivity
$\rightarrow$ anomalous skin effect

So, how good is Cu at low T?

$$R_s(l \to \infty) = \left[\sqrt{3}\pi \left(\frac{\mu_0}{4\pi} \right)^2 \right]^{1/3} \omega^{2/3} \left(\frac{l}{\sigma} \right)^{1/3}$$

"Extreme" anomalous limit (OK for Cu in RF and low T)

$l / \sigma = 6.8 \times 10^{-16}\ \Omega \cdot \mathrm{m}^2$ for Cu

$$\frac{R_s(4.2\ \mathrm{K}, 1.5\ \mathrm{GHz})}{R_s(300\ \mathrm{K}, 1.5\ \mathrm{GHz})} \approx 0.14$$

Does not compensate for the refrigerator efficiency!!!

Superconductivity - reminder

The 3 Hallmarks of Superconductivity

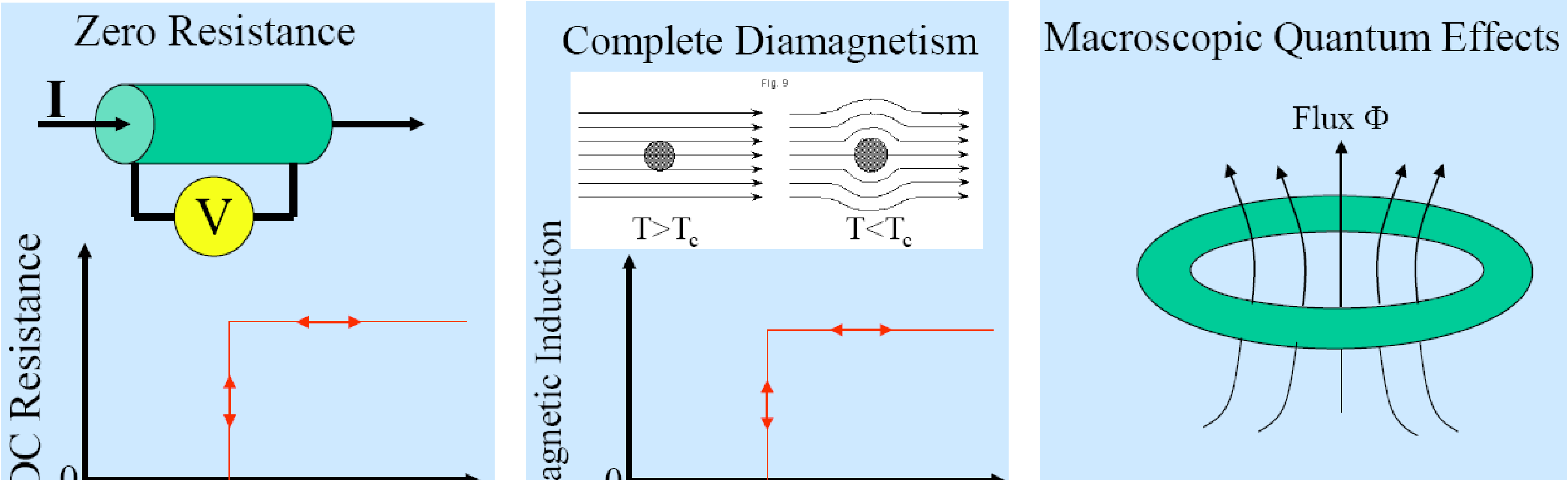

Flux quantization $\Phi = n\Phi_0$
Josephson Effects

London equations - Reminder

$$\frac{dJ_s}{dt} = \frac{1}{\mu_0 \lambda_L^2} E$$

- **E**=0: J_s goes on forever
- **E** is required to maintain an AC current

$$\nabla \times J_s = -\frac{1}{\mu_0 \lambda_L^2} B$$

- **B** is the source of J_s
- Spontaneus flux exclusion

$$\nabla^2 B = \frac{B}{\lambda_L^2}$$

Enter RF Superconductivity

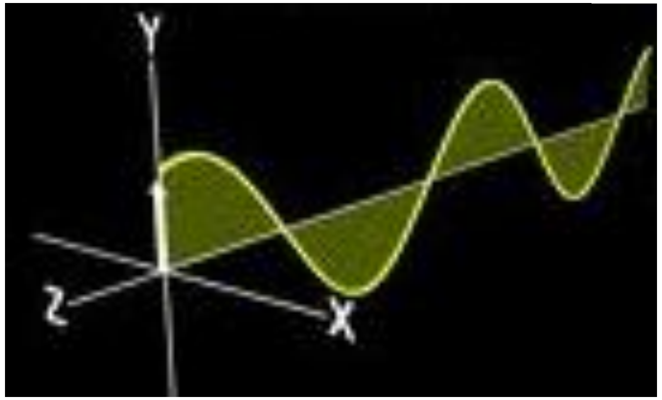

RF resistance is non zero

- In AC fields, the time-dependent magnetic field in the penetration depth will generate an electric field: $\vec{\nabla}\times\vec{E} = -\frac{\partial \vec{B}}{\partial t}$
- Because Cooper pairs have inertia (mass=2m_e) they cannot completely shield nc electrons from this E-field → $R_s > 0$

Materials provide boundary conditions with finite power dissipation

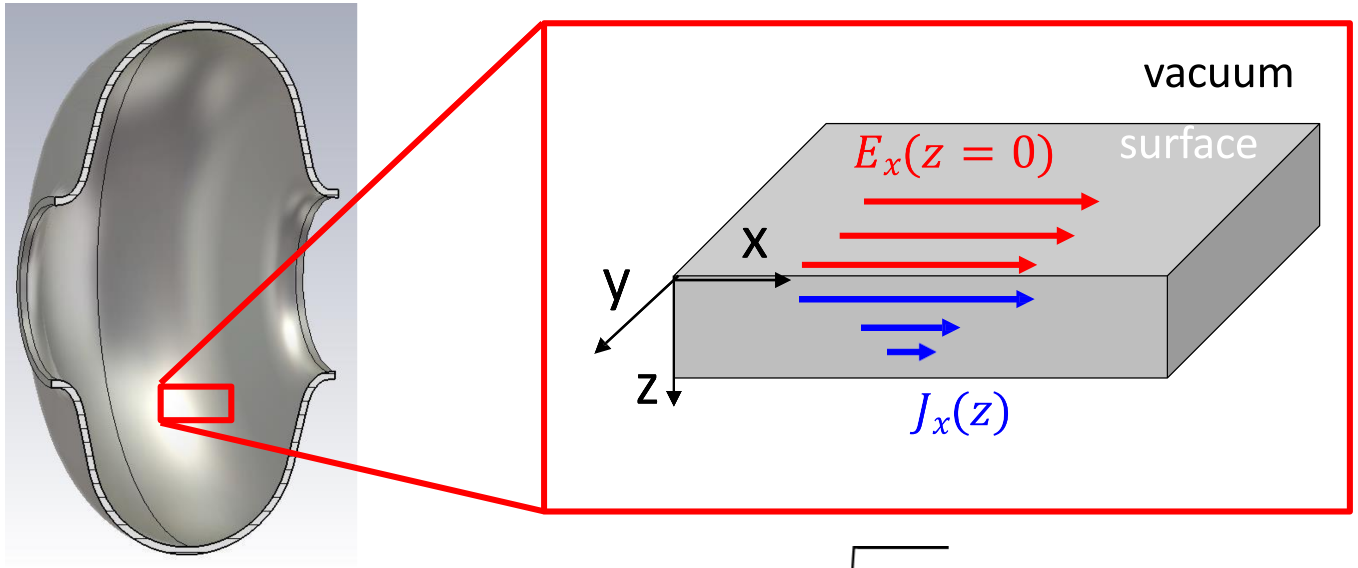

Normal conducting (Cu) $R_s = \sqrt{\frac{\pi f \mu_0}{\sigma}} \propto f^{1/2}$

Superconducting (Nb) $R_s = \frac{A f^2}{T}\exp\left(-\frac{\Delta}{k_B T}\right) \propto f^2$

Superconducting R_s is small but non zero

Local surface resistance

$$R_s \equiv \mathrm{Re}\left(\frac{E_x(z=0)}{\int_0^\infty J_x(z)dz}\right)$$

So, how does R_s for a superconductor compare to that of a normal conductor?

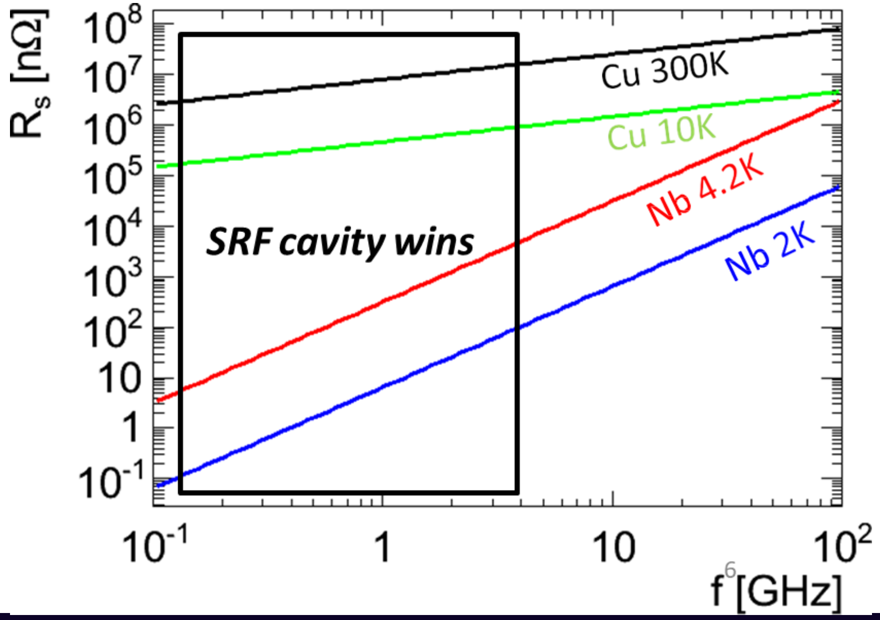

Two-fluid model

- Gorter and Casimir (1934) two-fluid model: charge carriers are divided in two subsystems, superconducting carriers of density $\mathbf{n_s}$ and normal electrons of density $\mathbf{n_n}$.
- The superconducting carriers are the Cooper pairs (1956) with charge -2e and mass 2m
- The normal current $\mathbf{J_n}$ and the supercurrent $\mathbf{J_s}$ are assumed to flow in parallel. J_s flows with no resistance.

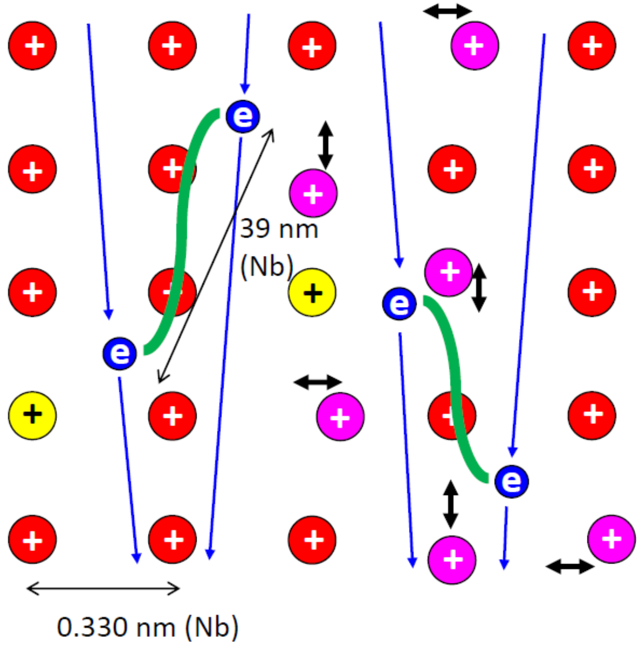

$$J = J_n + J_s$$

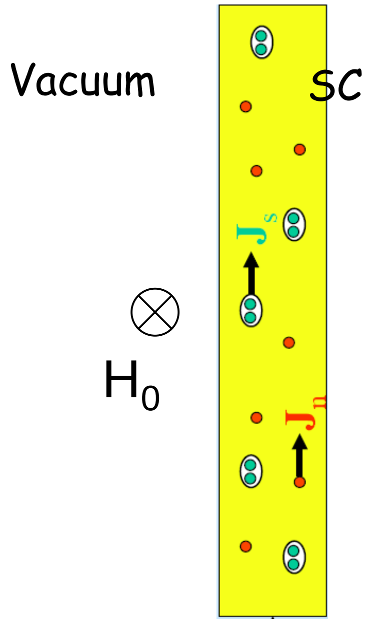

Electrodynamics of superconductors (at low field)

- London equations:

$$\frac{\partial}{\partial t}\vec{J}_s = \frac{\vec{E}}{\mu_0 \lambda_L^2}$$

$$\nabla \times \vec{J}_s = -\frac{1}{\lambda_L^2}\vec{H}$$

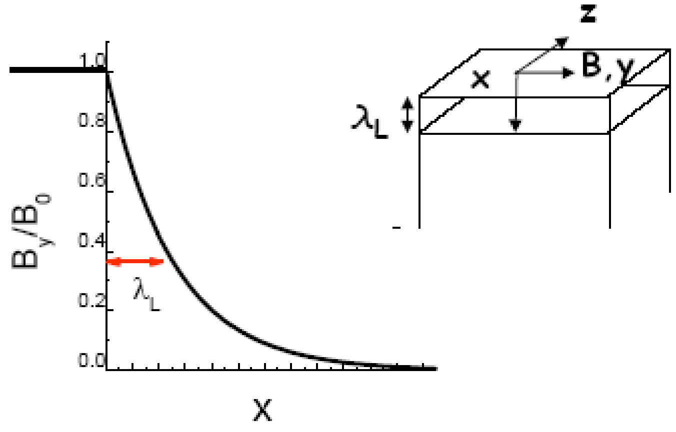

$$\boxed{\lambda_L = \sqrt{\frac{m}{\mu_0 n_s e^2}}}$$

London penetration depth

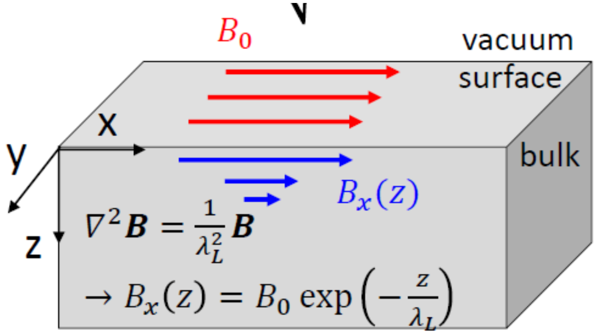

How much magnetic fields can penetrate into a superconductor

$\lambda_L \sim$ **36 nm** for Nb

- Currents and magnetic fields in superconductors can exist only within a layer of thickness λ_L

Note:

$$\vec{J}_s = -\frac{1}{\lambda_L^2}\vec{A}.$$

Local condition between current and field. Valid if $\xi_0 << \lambda_L$ or $l << \lambda_L$

Surface impedance of superconductors

$$\frac{\partial}{\partial t}\vec{J}_s = \frac{\vec{E}}{\mu_0 \lambda_L^2} \;\Rightarrow\; J_s = -i\underbrace{\frac{1}{\omega\mu_0\lambda_L^2}}_{=\,\sigma_2}E \;\Rightarrow\; J = J_n + J_s = \underbrace{(\sigma_1 - i\sigma_2)}_{\sigma}E$$

$$\sigma_1 = \sigma_n = \frac{n_n e^2 \tau}{m}, \quad \sigma_2 = \frac{n_s e^2}{m\omega}$$

- Electrodynamics of sc is the same as nc, only that we have to change $\sigma \rightarrow \sigma_1 - i\,\sigma_2$

- Penetration depth:

$$\delta = \sqrt{\frac{2}{\mu_0\sigma\omega}} = \frac{1}{\sqrt{\mu_0\omega\sigma_2}}\sqrt{\frac{2i}{1-i\,\sigma_1/\sigma_2}} \cong (1+i)\lambda_L\left(1+i\frac{\sigma_1}{2\sigma_2}\right)$$

$\sigma_1 << \sigma_2$ for sc at $T<<T_c$

$$H_y = H_0 \exp\left(-\frac{(1+i)}{\delta}x\right)$$

$$\boxed{H_y = H_0 e^{-\frac{x}{\lambda L}} e^{-i\frac{x}{\lambda L}\frac{\sigma 1}{2\sigma 2}}}$$

For Nb, λ_L = 36 nm, compared to δ = 1.7 μm for Cu at 1.5 GHz

Surface impedance of superconductors

$$Z_s = \sqrt{\frac{i\omega\mu_0}{\sigma}} = \sqrt{\frac{\omega\mu_0}{2\sigma_1}}(\varphi_- + i\varphi_+)$$

$$\varphi_\pm^2 = \frac{y}{1+y^2}\left(\sqrt{1+y^2} \pm 1\right) \qquad y = \frac{\sigma_1}{\sigma_2}$$

For a sc $\sigma_1 << \sigma_2 \rightarrow y << 1$ ➡ $\varphi_- = \sqrt{\frac{y^3}{2}}, \quad \varphi_+ = \sqrt{2y}$

$$X_s = \omega\underbrace{\mu_0\lambda_L}_{L_s}$$

L_s: kinetic inductance

$$Z_s = R_s + iX_s$$

$$R_s = \frac{1}{2}\mu_0^2\omega^2\sigma_1\lambda_L^3$$

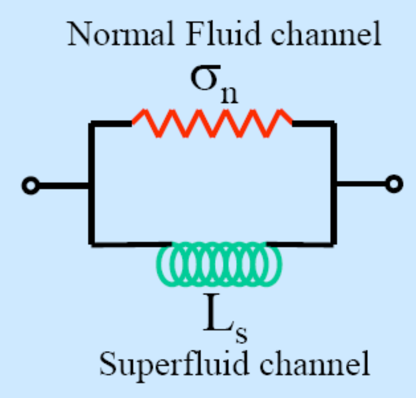

Surface resistance of superconductor

$$R_s = \frac{1}{2}\mu_0^2\omega^2\sigma_1\lambda_L^3$$

- $R_s \propto \sigma_1 \propto l \rightarrow$ longer m.f.p (higher conductivity) of unpaired e^- results in higher R_s !

- $R_s \propto \omega^2 \rightarrow$ use low-frequency cavities to reduce power dissipation
- Temperature dependence:

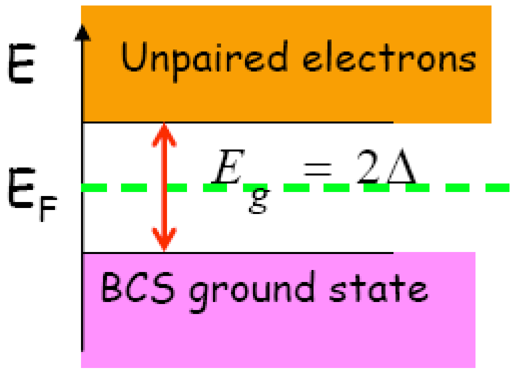

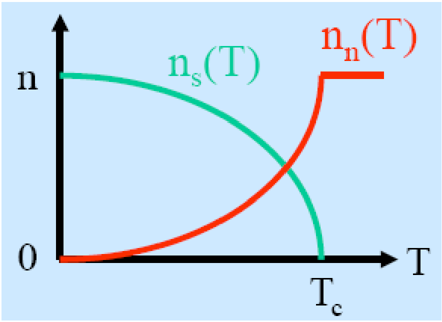

$n_s(T) \propto 1-(T/T_c)^4$

$\sigma_1(T) \propto n_n(T) \propto e^{-\Delta/k_B T}$

Unpaired electrons are created by the thermal breakup of Cooper pairs

$$R_s \propto \omega^2\lambda_L^3 l \exp(-\Delta/k_B T) \qquad T < T_c/2$$

Material purity dependence of R_s

- If $\xi_0 >> \lambda_L$ and $l >> \lambda_L$, the local relation between current and field is not valid anymore (similarly to anomalous skin effect in normal conductors)

Pippard (1953):

$$\vec{J}_s(\vec{r}) = -\frac{3}{4\pi\xi_0\lambda_L^2}\int_V \frac{\vec{R}\vec{R}\cdot\vec{A}(\vec{r}')e^{-R/\xi}}{R^4}d\vec{r}'$$

$$\frac{1}{\xi} = \frac{1}{\xi_0} + \frac{1}{l}$$

- The dependence of the penetration depth on l is approximated as

$$\lambda(l) \approx \lambda_L \sqrt{1+\frac{\xi_0}{l}}$$

$$\Rightarrow R_s \propto \left(1+\frac{\xi_0}{l}\right)^{3/2} l \Rightarrow$$

$R_s \propto l$ if $l >> \xi_0$ ("clean" limit)

$R_s \propto l^{-1/2}$ if $l << \xi_0$ ("dirty" limit)

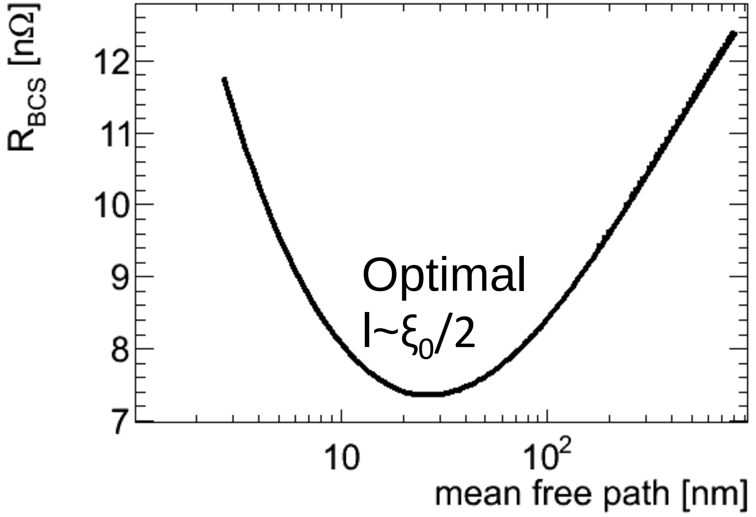

$\boxed{R_s \text{ has a minimum for } l = \xi_0/2}$

BCS surface resistance (1)

- From BCS theory of sc, Mattis and Bardeen (1958) have derived a non-local equation between the total current density **J** and the vector potential **A**

$$\vec{J}(\vec{r}) = \frac{3}{4\pi^2 v_0 \hbar \lambda_{L0}^2} \int_V \frac{\vec{R}\vec{R}\cdot\vec{A}(\vec{r}')I(\omega,R,T)e^{-R/l}}{R^4} d\vec{r}'$$

can be converted in a product in Fourier domain:

$J(q) = -K(q)A(q)$

- The surface impedance can be derived in term of the Kernel $K(q)$:

$$Z_s = \frac{j\mu_0\omega\pi}{\int_0^\infty \ln\left(1+\frac{K(q)}{q^2}\right)dq}$$

for diffuse scattering of electrons at the metal surface

$$\begin{aligned}
\mathrm{Re}\{\mathrm{K(q)}\} &= \frac{3}{\hbar \mathrm{v}_0 \lambda_{\mathrm{L0}}^2 \mathrm{q}} \times \\
&\Bigg\{ \int_{\max\{\Delta-\hbar\omega,-\Delta\}}^{\Delta} [1-2f(E+\hbar\omega)]\{\frac{E^2+\Delta^2+\hbar\omega E}{\sqrt{\Delta^2-E^2}\sqrt{(E+\hbar\omega)^2-\Delta^2}} R(a_2,a_1+b)+S(a_2,a_1+b)\}dE \\
&+ \frac{1}{2}\int_{\Delta-\hbar\omega}^{-\Delta} [1-2f(E+\hbar\omega)]\{[g(E)+1]S(a^-,b)-[g(E)-1]S(a^+,b)\}dE \\
&- \int_{\Delta}^{\infty} [1-f(E)-f(E+\hbar\omega)][g(E)-1]S(a^+,b)dE \\
&+ \int_{\Delta}^{\infty} [f(E)-f(E+\hbar\omega)][g(E)+1]S(a^-,b)dE \Bigg\}
\end{aligned}$$

$$\begin{aligned}
\mathrm{Im}\{\mathrm{K(q)}\} &= \frac{3}{\hbar \mathrm{v}_0 \lambda_{\mathrm{L0}}^2 \mathrm{q}} \times \\
&\Bigg\{ -\frac{1}{2}\int_{\Delta-\hbar\omega}^{-\Delta} [1-2f(E+\hbar\omega)]\{[g(E)+1]R(a^-,b)+[g(E)-1]R(a^+,b)\}dE \\
&+ \int_{\Delta}^{\infty} [f(E)-f(E+\hbar\omega)]\{[g(E)+1]R(a^-,b)+[g(E)-1]R(a^+,b)\}dE \Bigg\}
\end{aligned}$$

BCS surface resistance (2)

- There are numerical codes (Halbritter (1970)) to calculate R_{BCS} as a function of ω, T and material parameters (ξ_0, λ_L, T_c, Δ, l)
- For example, check http://www.lepp.cornell.edu/~liepe/webpage/researchsrimp.html

- A good approximation of R_{BCS} for $T < T_c/2$ and $\omega < \Delta/\hbar$ is:

$$R_{BCS} \cong \frac{\mu_0^2 \omega^2 \lambda^3 \sigma_n \Delta}{k_B T} \ln\left[\frac{C_1 k_B T}{\hbar\omega}\right] \exp\left[-\frac{\Delta}{k_B T}\right] \qquad C_1 = 2.246$$

Let's run some numbers: Nb at 2.0 K, 1.5 GHz $\rightarrow$ λ = 40 nm,
$\sigma_n = 3.3\times10^8$ 1/Ωm, $\Delta/k_B T_c = 1.85$, $T_c = 9.25$ K

$R_{BCS} \cong 20$ nΩ $\qquad$ $X_s \cong 0.47$ mΩ

$$\begin{array}{l} \text{Nb} \rightarrow \\ \text{Cu} \rightarrow \end{array} \frac{R_{BCS}(2\,\text{K}, 1.5\,\text{GHz})}{R_s(300\,\text{K}, 1.5\,\text{GHz})} \cong 2\times10^{-6}$$

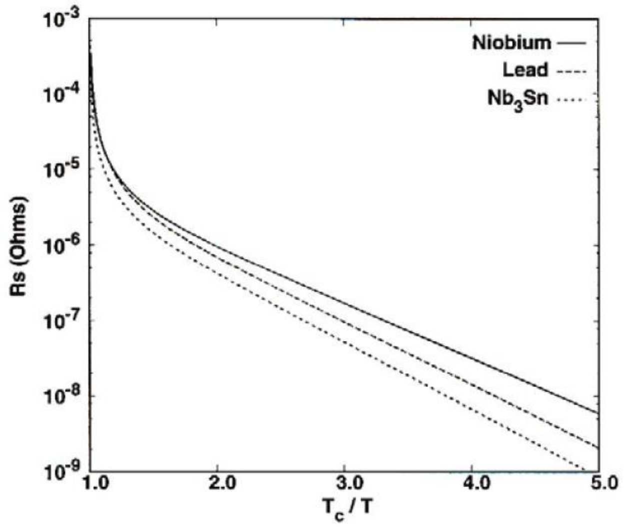

Figure 4.5: Theoretical surface resistance at 1.5 GHz of lead, niobium and Nb_3Sn as calculated from program [94]. The values given in Table 4.1 were used for the material parameters.

Not so fast…

- Refrigeration isn't free:

Carnot efficiency: η_C = 2 K/(300 K – 2 K) = 0.007

Technical efficiency of cryoplant: $\eta_T \cong 0.2$

➡ Total efficiency: $\eta_{tot} \cong 0.0014 \cong 1/700$

➡ Power reduction from Cu(300K) to Nb(2K) is $\cong$ $\mathbf{10^3}$

SRF Material Requirements

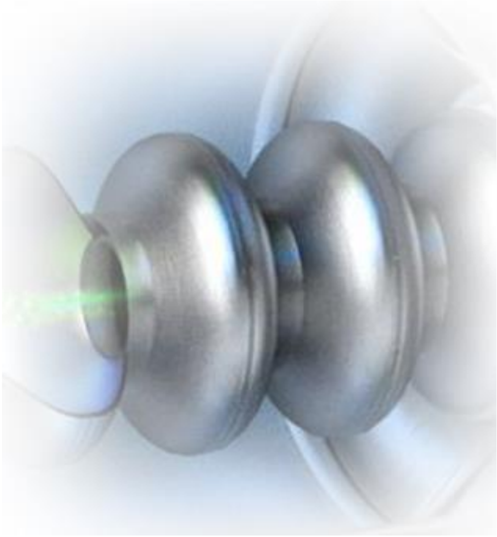

- ❑ Low surface resistance, including low residual resistance.

Superconducting cavities are dominated by their surface quality (Niobium & other SC)

- ❑ S-wave Cooper pairing with a full superconducting gap on the entire Fermi surface.
- ❑ High lower critical magnetic field H_{c1} and superheating magnetic H_{SH}

difficult to reach in real "accelerating cavities" (low T, large scale cavity fabrication, surface defects,…)

- ❑ High thermal conductivity.
- ❑ Grain boundaries transparent to high RF screening currents in polycrystalline material.
- ❑ Minimal degradation of superconducting properties by local chemical non-stoichiometry and precipitation of non-superconducting second phases.
- ❑ Good formability & sustainability to fabrication/preparation processes

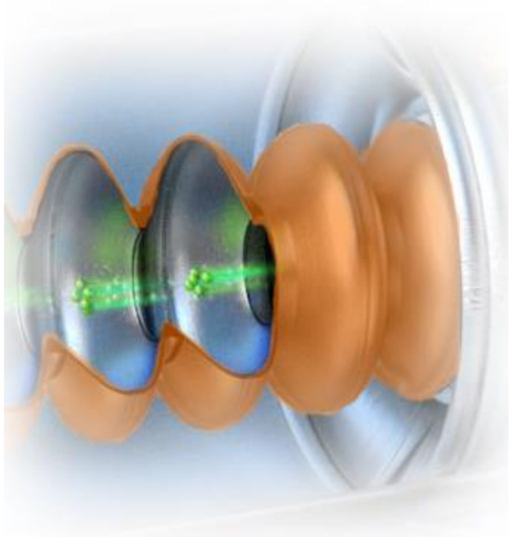

Various Superconducting materials – only one practical and commonly used

Superconductor	λ_L (0) (nm)	ξ_0 (nm)	κ	$2\Delta(0)/kT_c$	T_c(K)
Al	16	1500	0.011	3.40	1.18
In	25	400	0.062	3.50	3.3
Sn	28	300	0.093	3.55	3.7
Pb	28	110	0.255	4.10	7.2
Nb	32	39	0.82	3.5-3.85	8.95-9.2
Ta	35	93	0.38	3.55	4.46
Nb_3Sn	50	6	8.3	4.4	18
NbN	50	6	8.3	4.3	≤17
$Yba_2Cu_3o_x$	140	1.5	93	4.5	90

"Superheating" field for niobium at 0 K is 2.4 kGauss

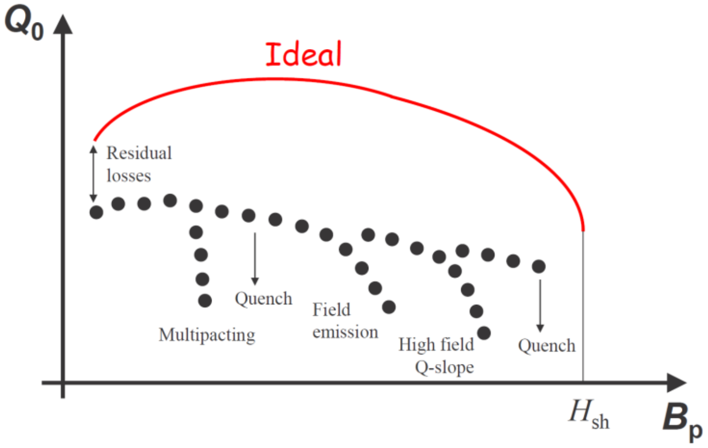

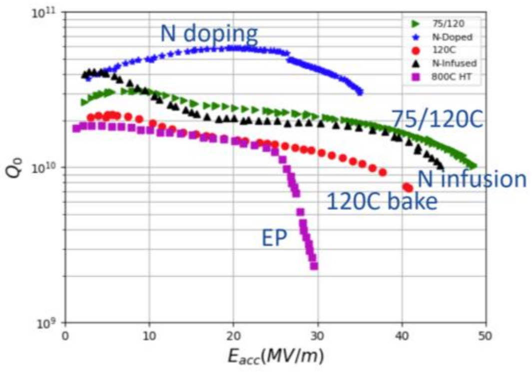

Currently Nb provides the best compromise to all requirements.

- ❑ Low surface resistance, including low residual resistance.
- ❑ S-wave Cooper pairing with a full superconducting gap on the entire Fermi surface.
- ❑ High lower critical magnetic field H_{c1} and superheating magnetic H_{SH}
- ❑ High thermal conductivity.
- ❑ Uniform composition, no phase transition in the domain of interest
- ❑ Very large ξ: makes it less sensitive to small crystalline defects (e.g. GB)
- ❑ Grain boundaries transparent to high RF screening currents in polycrystalline material.
- ❑ Minimal degradation of superconducting properties by local chemical non-stoichiometry and precipitation of non-superconducting second phases.
- ❑ Good formability

Experimental results

Frequency dependence

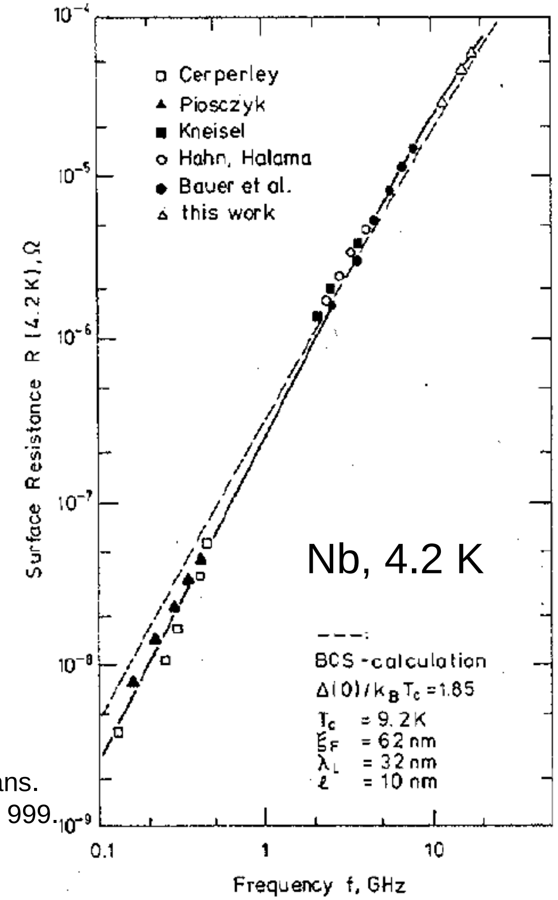

A. Phillip and J. Halbritter, IEEE Trans. Magn. **19**(3) (1983) 999.

- Small deviations from BCS theory can be explained by strong coupling effects, anisotropic energy gap in the presence of impurity scattering or by inhomogeneities

Dependence on material purity

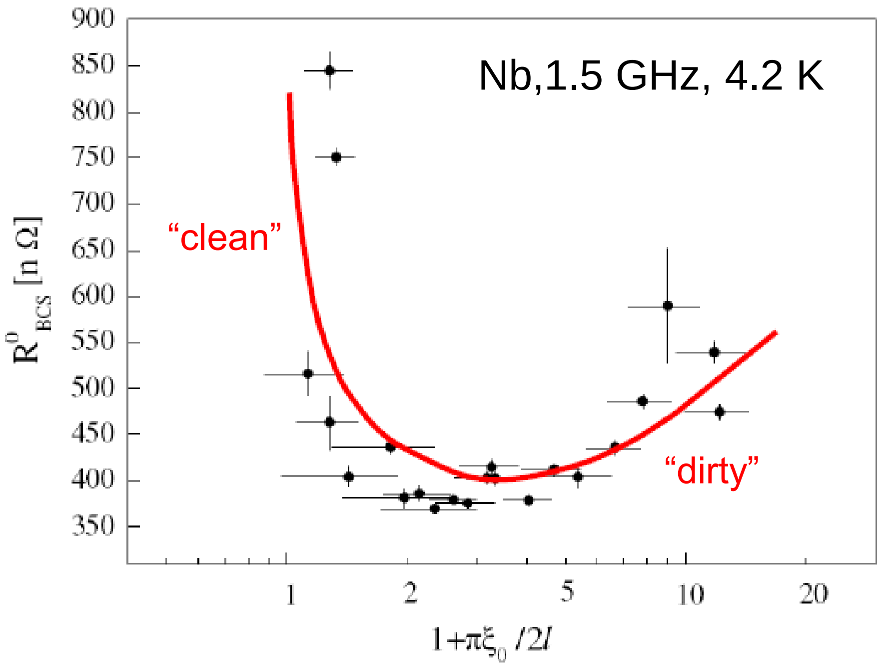

C. Benvenuti et al., Physica C **316** (1999) 153.

- Nb films sputtered on Cu
- By changing the sputtering species, the mean free path was varied

R_{BCS} can be optimized by tuning the density of impurities at the cavity surface.

Residual resistance

$$R_s = R_{BCS}(\omega, T, \Delta, T_c, \lambda_L, \xi_0, l) + R_{res}(?)$$

Possible contributions to R_{res}:

- Trapped magnetic field
- Normal conducting precipitates
- Grain boundaries
- Interface losses
- Subgap states

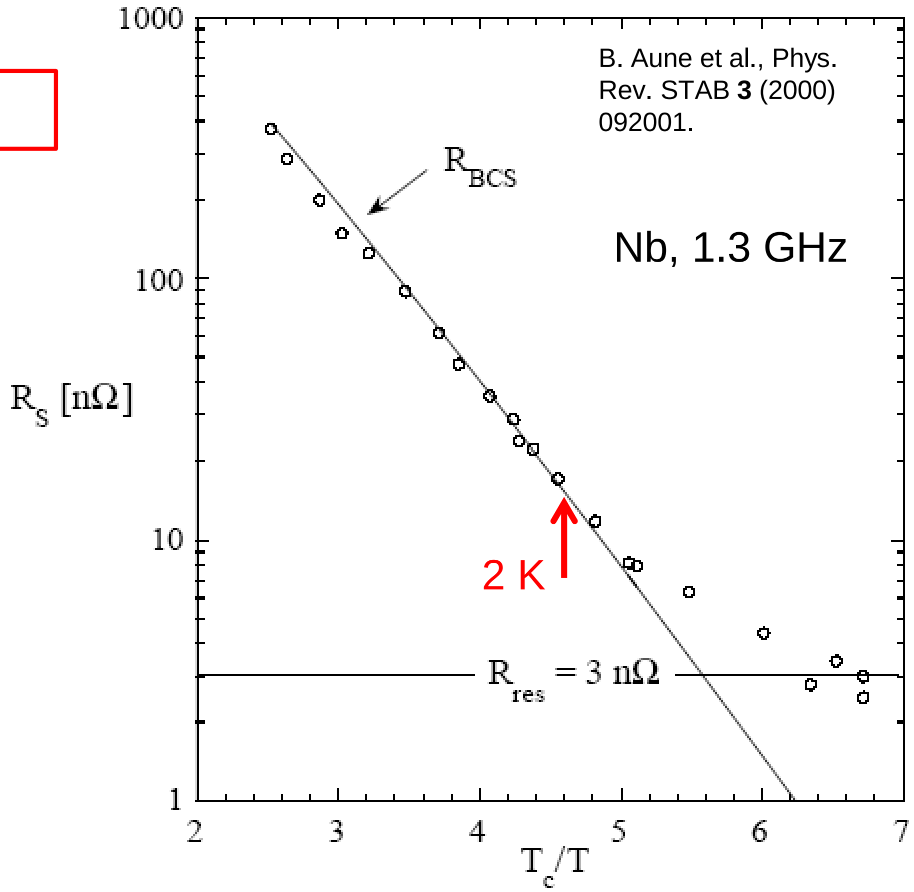

For Nb, R_{res} (~1-10 nΩ) dominates R_s at low frequency (*f* < ~750 MHz) and low temperature (T < ~2.1 K)

Possible contributions to R_{res} in Nb (1)

Jefferson Lab

- Trapped magnetic field

In technical materials, the Meissner effect is incomplete when cooling below T_c in the presence of a residual magnetic field due to pinning

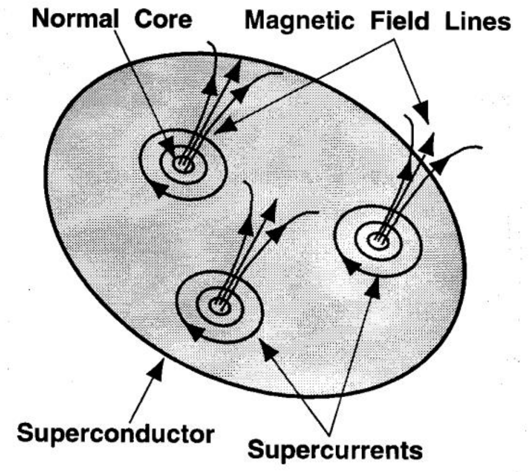

Fluxoids: normal conducting core of area $\sim\pi\xi_0^2$ and normal-state surface resistance, R_n

$$R_{res} = N\frac{\pi\xi_0^2}{A}R_n$$

$$N = \mu_0 H_{ext}/\Phi_0 \quad \text{if 100\% flux pinning}$$

$$= \frac{H_{ext}\pi\xi_0^2\mu_0}{\Phi_0}R_n = \frac{H_{ext}}{2H_{c2}}R_n$$

$$H_{c2} = \frac{\Phi_0}{2\pi\mu_0\xi_0^2}$$

$$\boxed{R_{res} \cong 0.2(\mathrm{n\Omega})H_{ext}(\mathrm{mOe})\sqrt{f\,(\mathrm{GHz})}}$$

R_{res} due to Earth's field (~500 mG) at 1.5 GHz: ~120 nΩ (~6×R_{BCS}(2K))

→ Apply magnetic shielding around cavities

Possible contributions to R_{res} in Nb (2)

- Trapped magnetic field

Including the oscillatory motion of a fluxoid due to the Lorentz force:

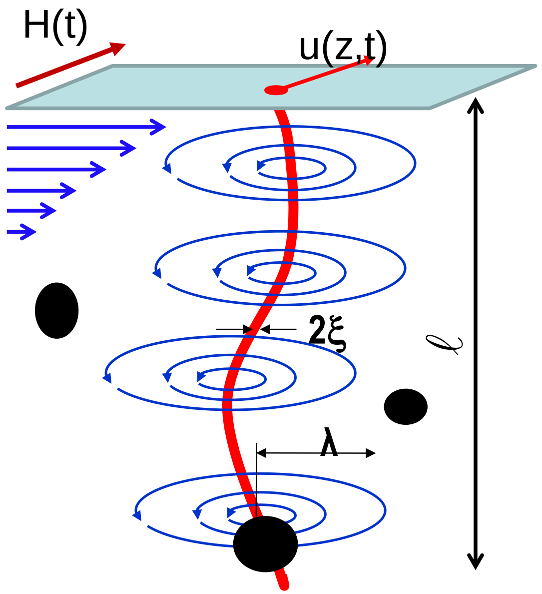

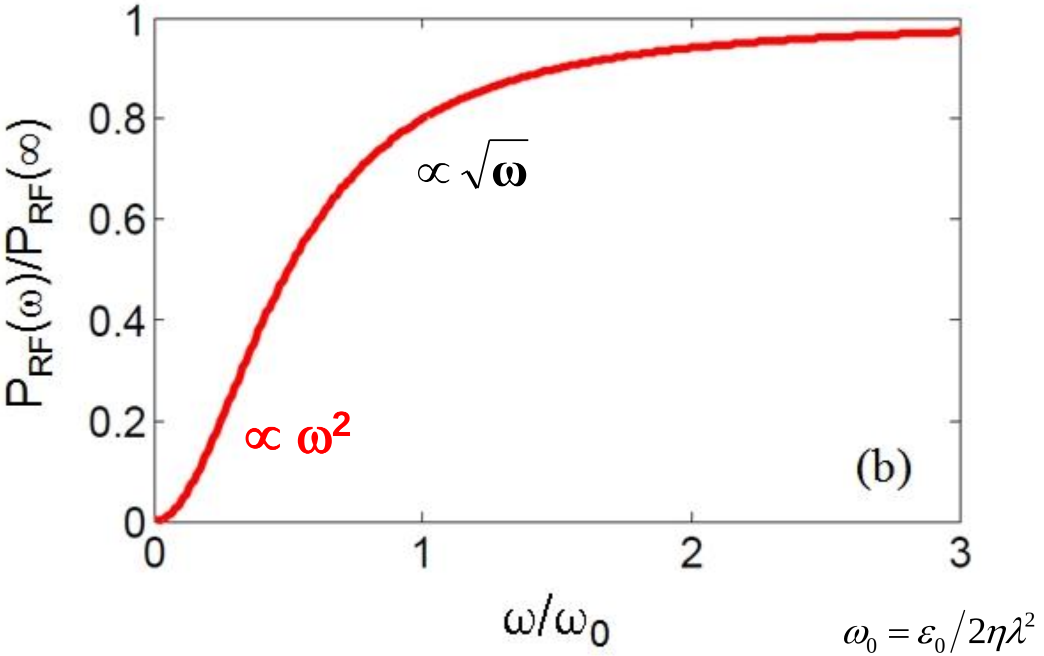

$\omega_0 = \varepsilon_0 / 2\eta\lambda^2$

A. Gurevich and G. Ciovati, Phys. Rev. B. **87,** 054502 (2013)

In the frequency limit where only the tip of the fluxoid vibrates $R_{res} = \dfrac{H_{ext}}{H_c}\dfrac{R_n}{\sqrt{g}}$

$g = \dfrac{1}{\Gamma^2}\ln(\Gamma\kappa_{GL}) + \dfrac{1}{2}$ $\quad \Gamma = \dfrac{\lambda_c}{\lambda}$ Anisotropy parameter

For Nb: ρ_n~5×10^{-10} Ωm, H_c=2000 Oe, 2g=1

$$\boxed{R_{res} \cong 1(\mathrm{n}\Omega) H_{ext}(\mathrm{mOe})\sqrt{f(\mathrm{GHz})}}$$

Possible contributions to R_{res} in Nb (3)

- Normal conducting precipitates

If the bulk H content in high-purity (RRR~300) Nb is > ~5 wt.ppm, precipitation of normal-conducting NbH_x islands occurs at the surface if the cooldown rate is < ~1 K/min in the region 75-150 K

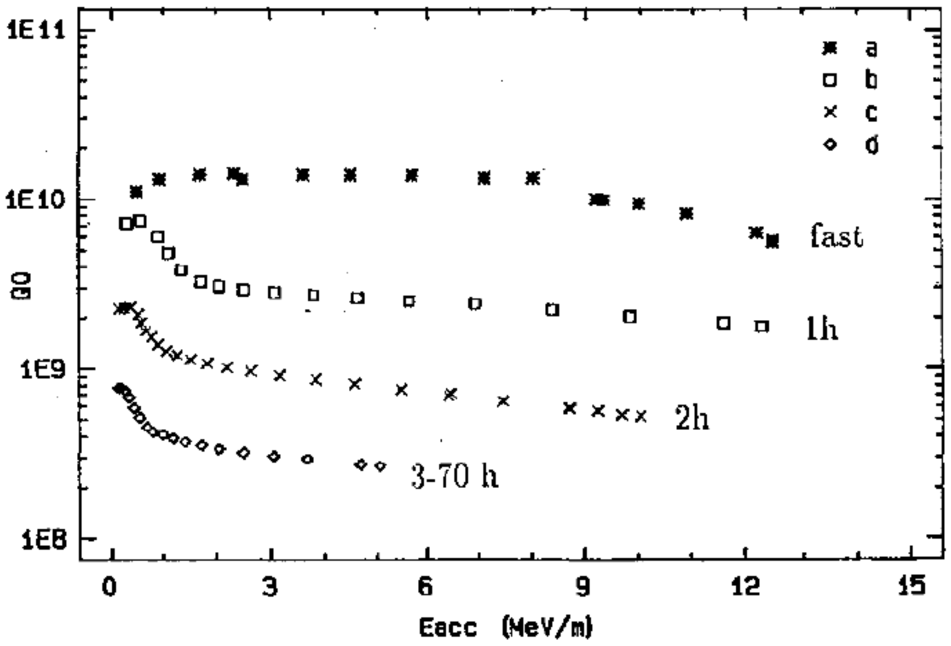

B. Aune et al., Proc. 1990 LINAC Conf. (1990) 253.

Nb cavities are heat treated at 600 – 800 °C in a UHV furnace to degas H

Possible contributions to R_{res} in Nb (4)

- Subgap states
- Grain boundaries → Results are still inconclusive
- Interface losses → Results are still inconclusive

Tunneling measurements show that the BCS singularity in the electronic density of states is smeared out and subgap states with finite $N(\varepsilon)$ appear at energies below Δ.

Phenomenological formula [ ]:

$$N(\epsilon) = \mathrm{Re}\frac{N_n(\epsilon - i\gamma)}{\sqrt{(\epsilon - i\gamma)^2 - \Delta^2}}$$

γ: damping parameter

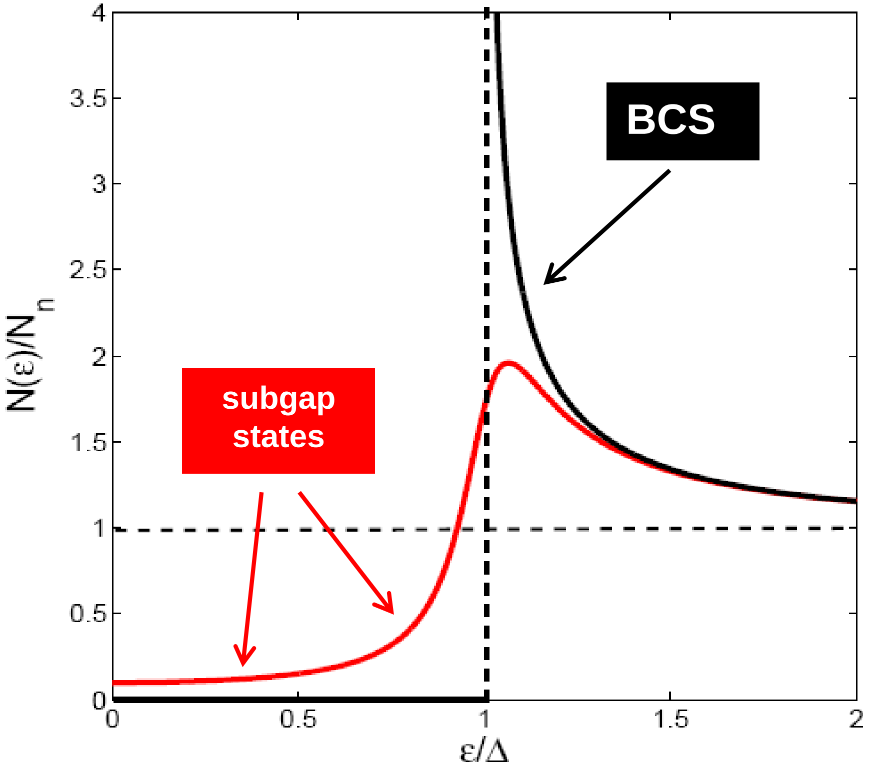

Finite density of states at the Fermi level:

$$N(0) \simeq \gamma N_n / \Delta$$

Residual resistance ($\sigma_1 \rightarrow \sigma_n\gamma/\Delta$):

$$R_{res} \approx \mu_0^2 \omega^2 \lambda^3 \sigma_n \gamma / \Delta$$

R_{res} ~10 nΩ at 1.5 GHz for $\gamma/\Delta = 10^{-3}$

A. Gurevich, Rev. Accel. Sci. Tech. **5,** 119 (2012)

About HTS…

LTS

HTS

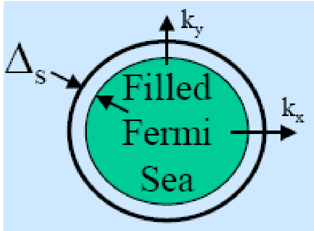

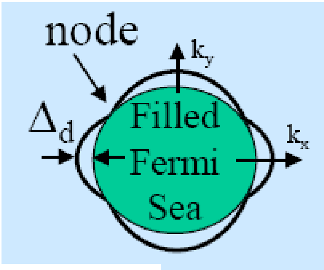

- HTS materials have nodes in the energy gap. This leads to **power-law** behavior of $\lambda(T)$ and $R_s(T)$ and **high** residual losses

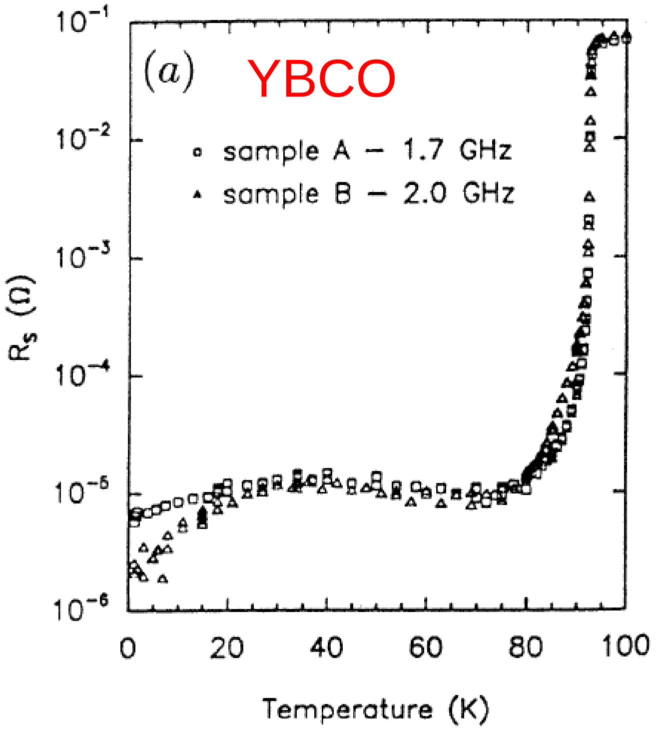

Hein M A 1996 *Studies in High Temperature Superconductors* vol 18 ed A Narlikar (Nova Science Publishers) pp 141–216

- $\xi \sim 1 – 2$ nm ($<< \lambda$) $\rightarrow$ superconducting pairing is easily disrupted by defects (cracks, grain boundaries)
- "Granular" superconductors: high grain boundary resistance contributing to R_{res}

We are stuck with LHe!

Surface barrier

How do vortices get in a superconductor?

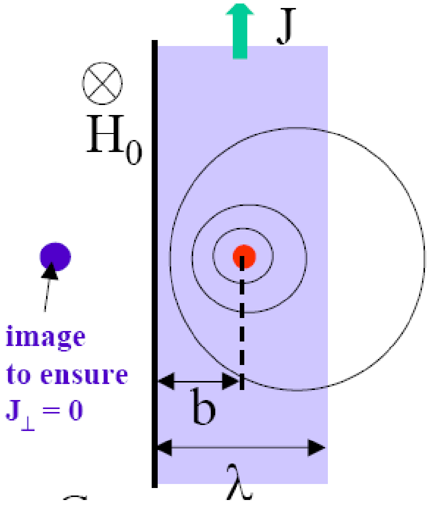

Two forces acting on the vortex at the surface:

- Meissner currents push the vortex in the bulk
- Attraction to the antivortex image pushes the vortex out

Thermodynamic potential *G*(*b*) as a function of the ˙tion *b*:

$$G(b) = \phi_0 [H_0 e^{-b/\lambda} - H_v(2b) + H_{c1} - H_0]$$

Meissner Image

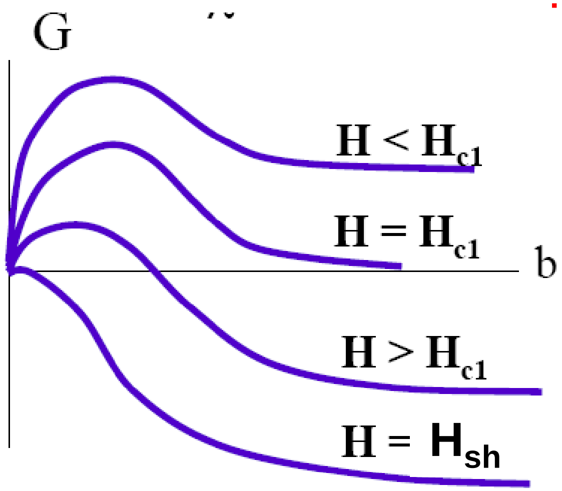

- Vortices have to overcome the surface barrier even at $H > H_{c1}$
- Surface barrier disappears only at $H=H_{sh}$
- Surface barrier is reduced by defects

What is the highest RF field applicable to a superconductor?

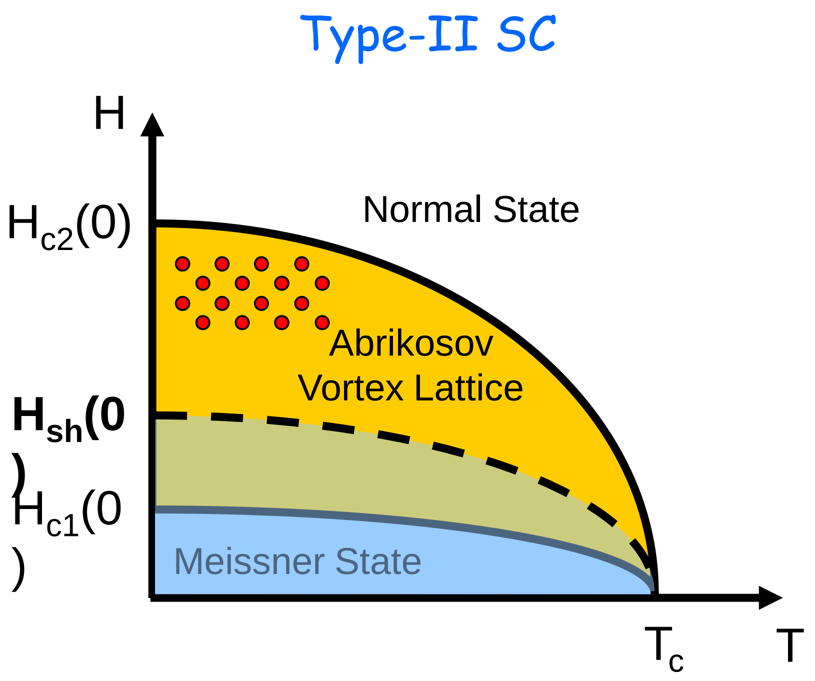

- Penetration and oscillation of vortices under the RF field gives rise to strong dissipation and the surface resistance of the order of R_s in the normal state
- the Meissner state can remain metastable at higher fields, $H > H_{c1}$ up to the superheating field H_{sh} at which the Bean-Livingston surface barrier for penetration of vortices disappears and the Meissner state becomes unstable

H_{sh} is the maximum magnetic field at which a type-II superconductor can remain in a true non-dissipative state not altered by dissipative motion of vortices.

At $H = H_{sh}$ the screening surface current reaches the depairing value $J_d = n_s e\Delta/p_F$

Superheating field: theory

Jefferson Lab

- Calculation of $H_{sh}(\kappa)$ from Ginzburg-Landau theory ($T \approx T_c$) [Matricon and Saint-James (1967)]:

$$H_{sh} \approx 1.2 H_c, \quad \kappa \cong 1$$
$$H_{sh} \approx 0.745 H_c, \quad \kappa >> 1$$

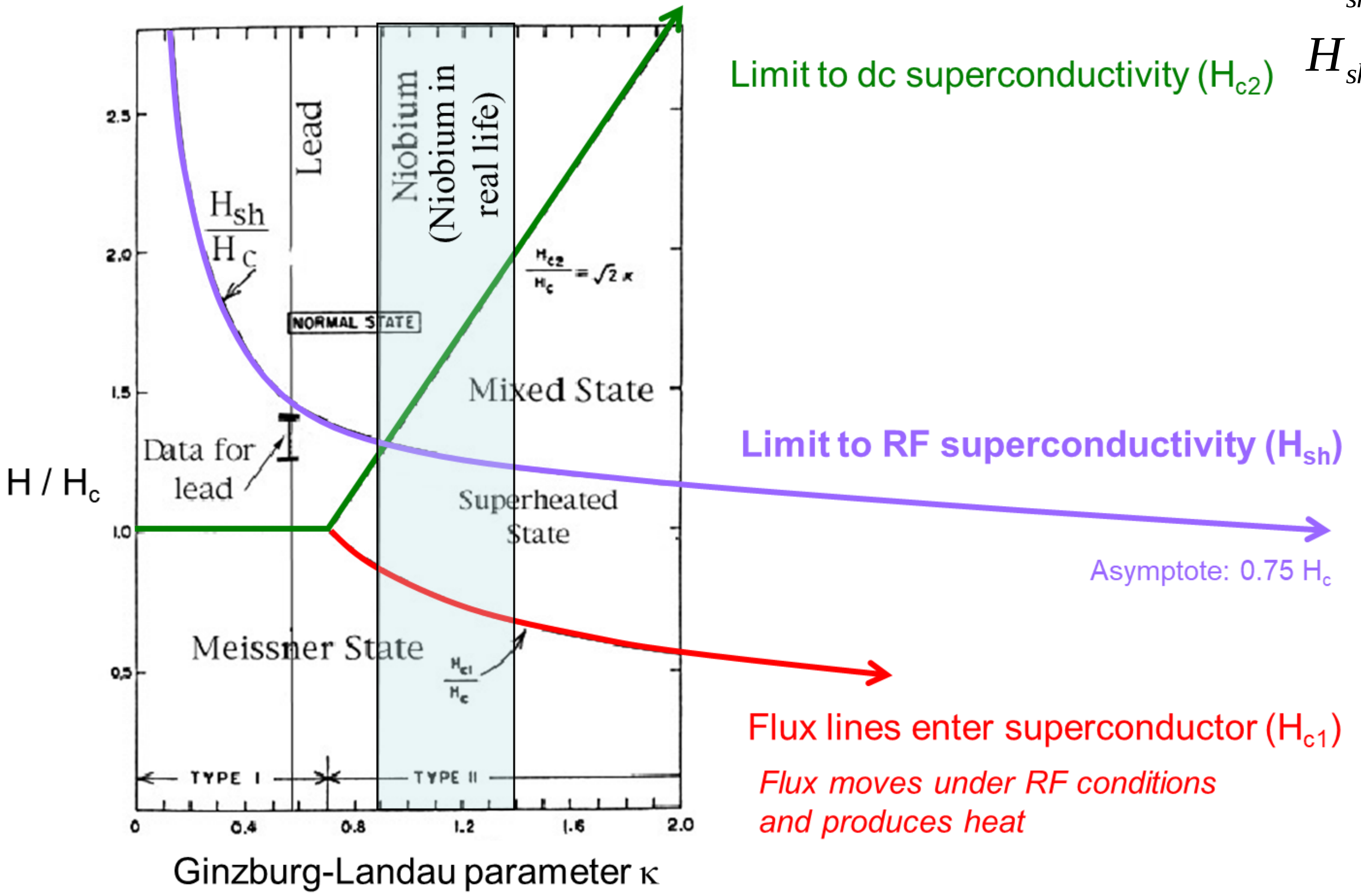

Plot from Padamsee

Time evolution of the spatial pattern of the order parameter in a small region around the boundary where a vortex entrance is taking place, calculated from time-dependent GL-equations. t

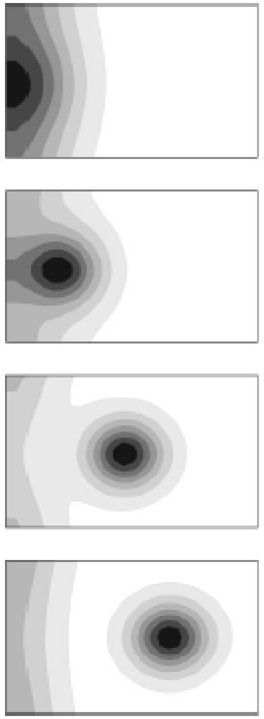

A. D. Hernandez and D. Dominguez, Phys. Rev. B **65**, 144529 (2002)

Alternative Materials to Nb

Jefferson Lab

Material	T_c (K)	H_c [T]	H_{c1} [mT]	H_{c2} [T]	$\lambda(0)$ [nm]	Δ [meV]
Nb	9.2	0.2	170	0.4	40	1.5
$B_{0.6}K_{0.4}BiO_3$	31	~0.44	30	30	160	4.4
Nb_3Sn	18	~0.5	40	30	85	3.1
NbN	16.2	~0.23	20	15	200	2.6
MgB_2	40	~0.32	20-60	3.5-60	140	2.3; 7.1
$Ba_{0.6}K_{0.4}Fe_2As_2$	38	~0.5	20	>100	200	>5.2

Example: 4 layers 30 nm thick of Nb_3Sn on Nb $\rightarrow$ H_a up to ~400 mT [~$H_{sh}(Nb_3Sn)$] with H_i ~ 100 mT << H_{sh}(Nb)

- Global surface resistance:

$$R_s = \left(1 - e^{-2Nd/\lambda}\right) R_0 + e^{-2Nd/\lambda} R_b$$

$R_0^{Nb3Sn}(2\text{ K}) \cong 0.1\, R_b^{Nb}(2\text{ K}) \rightarrow R_s \approx 0.15\, R_b$

Superheating field: experimental results

Use high-power (~1 MW) and short (~100 μs) RF pulses to achieve the metastable state before other loss mechanisms kick-in

Highest H_p ever measured in CW!!!

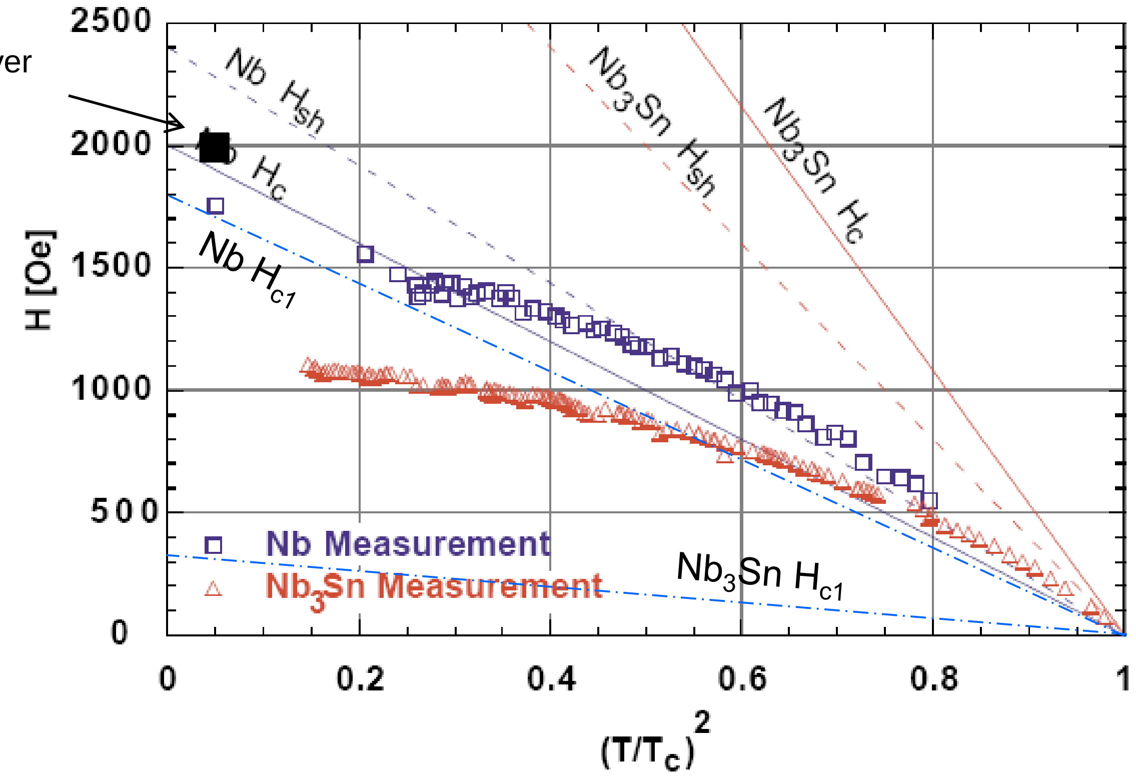

T. Hays and H. Padamsee, Proc. 1997 SRF Workshop, Abano Terme, Italy, p. 789 (1997) .

RF magnetic fields higher than H_{c1} have been measured in both Nb and Nb_3Sn cavities.

However max H_{RF} in Nb_3Sn is << predicted H_{sh}…

However…

- In "real" surfaces, the surface barrier can be easily suppressed locally by "defects" such as roughness or impurities, so that vortices may enter the sc already at $H_{RF} \approx H_{c1}$

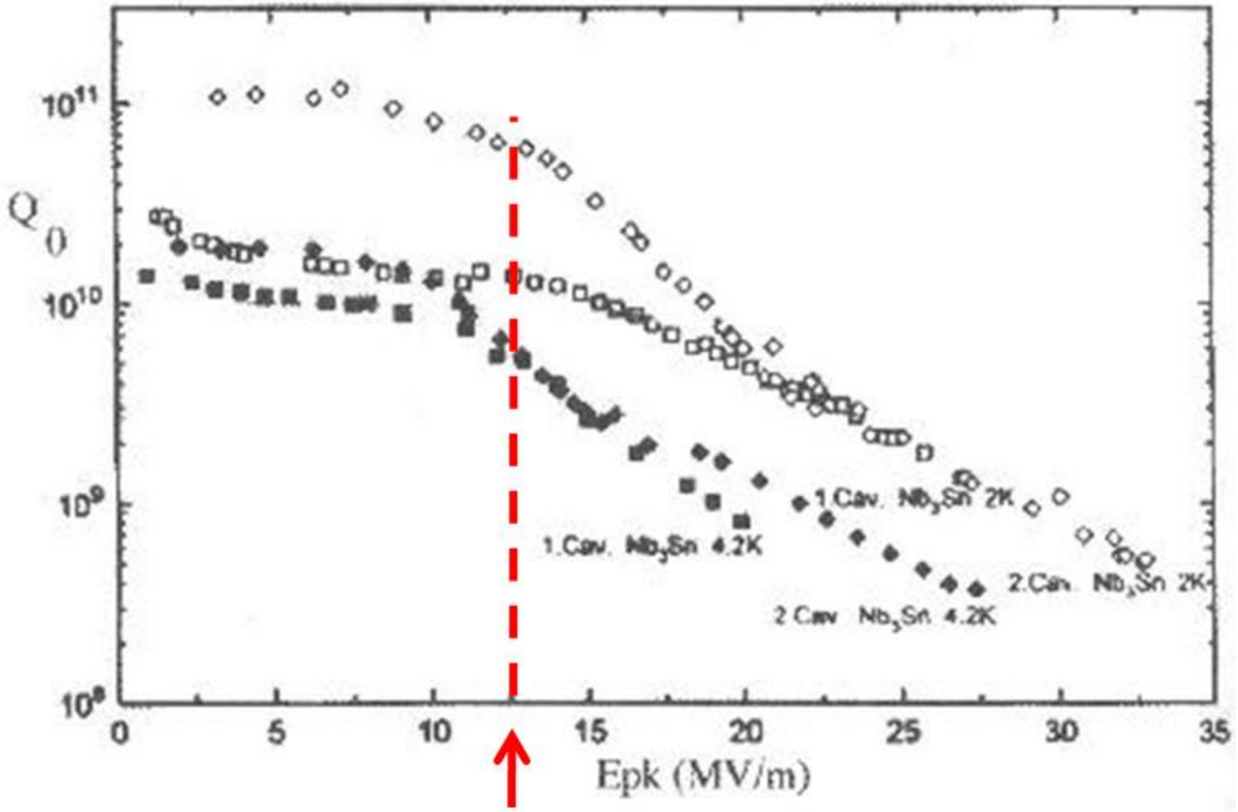

$H_p \sim 30\ mT \sim H_{c1}$

1.5 GHz, Nb_3Sn film deposited on Nb

G. Muller et al., Proc. 1996 EPAC, Spain, p. 2085 (1996)

Multilayer Films

- If H_{c1} is indeed a major practical limit for RF application of high-κ materials, a possible solution consists of S-I-S multilayers [Gurevich (2006)]:

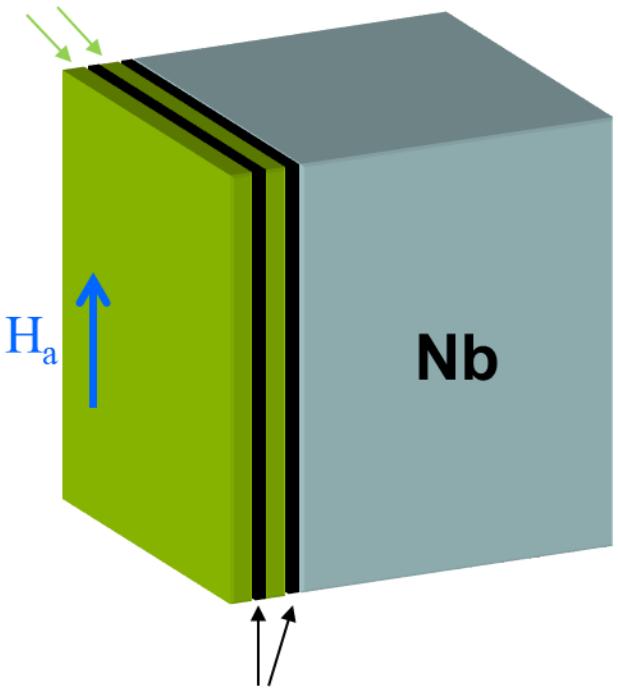

Suppression of vortex penetration due to the enhancement of H_{c1} in a thin film with $d < \lambda$

[Abrikosov, (1964)]

$$H_{c1} = \frac{2\phi_0}{\pi d^2}\left(\ln\frac{d}{\xi} - 0.07\right)$$

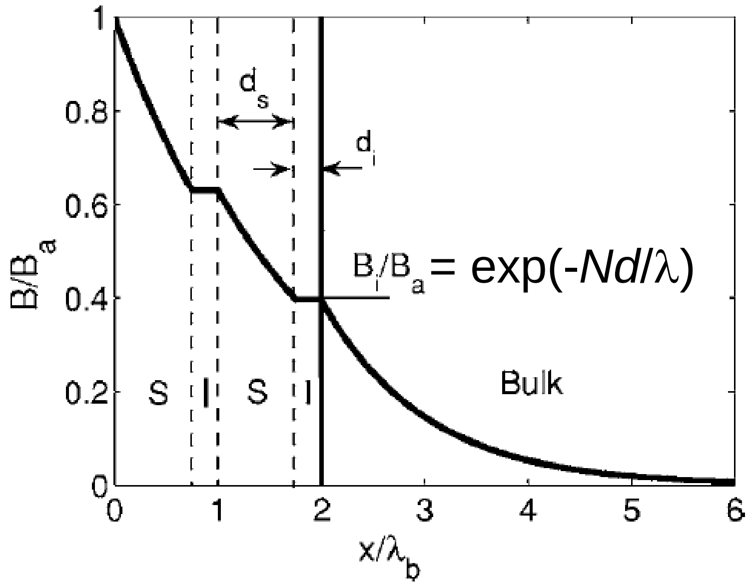

A. Gurevich, Appl. Phys. Lett. **88**, 012511 (2006)

Global thermal instability

- The exponential temperature dependence of $R_s(T)$ provides a strong positive feedback between RF Joule power and heat transport to the coolant → thermal instability above the breakdown field H_b

$$\frac{1}{2}R_s(T_m)H_0^2 = \int_{T_m}^{T_s}\kappa(T)dT = h_K(T_s,T_0)(T_s - T_0)$$

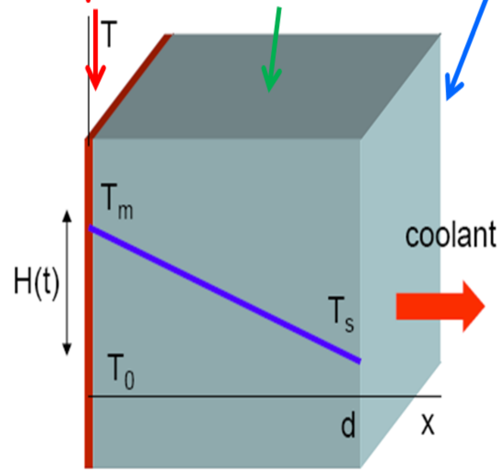

A. Gurevich, Physica C **441**, 38 (2006)

κ: thermal conductivity
h_K: Kapitza conductance

$T_m - T_0 << T_0$

$$\frac{1}{2}R_s(T_m)H_0^2 = \frac{h_K\kappa}{\kappa + dh_K}(T_m - T_0)$$

= α, total thermal conductance

Uniform thermal breakdown field

$$R_s(T_m) \cong \frac{A\omega^2}{T_m}e^{-\Delta/kT_m} + R_{res} \qquad H_0^2 = \frac{2\kappa h_K T_m(T_m - T_0)}{(\kappa + h_K d)\left[A\omega^2\exp(-\Delta/kT_m) + R_{res}T_m\right]}$$

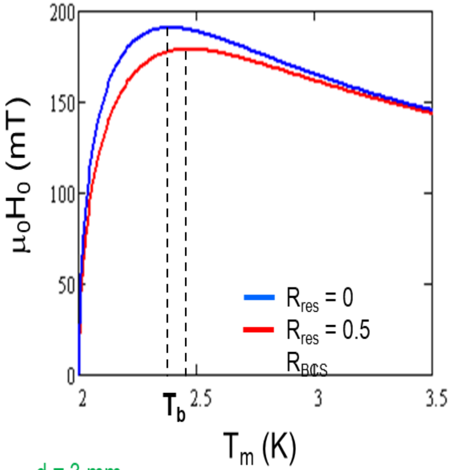

d = 3 mm
f = 1.5 GHz
$R_{BCS}(2\ K) = 20\ n\Omega$
$h_K = 5\ kW/m^2K$
$\kappa = 10\ W/mK$
$T_0 = 2\ K$
$\Delta/k = 17.1\ K$

$H_b = \max H_0(T_m) = H_0(T_b)$

$T_b - T_0 \approx T_0^2/\Delta T_c$ = 0.23 K for Nb

$R_{res} \cong 0$

← $\exp(-\Delta T_c/T_b) \approx \exp(-\Delta T_c/T_0 + 1)$

$$\boxed{H_b = \left[\frac{2kT_0^2 h_K\kappa}{(\kappa + dh_K)\Delta e R_{BCS}}\right]^{1/2}}$$

Uniform thermal breakdown field

Nb, 2 K, same parameters as previous slide

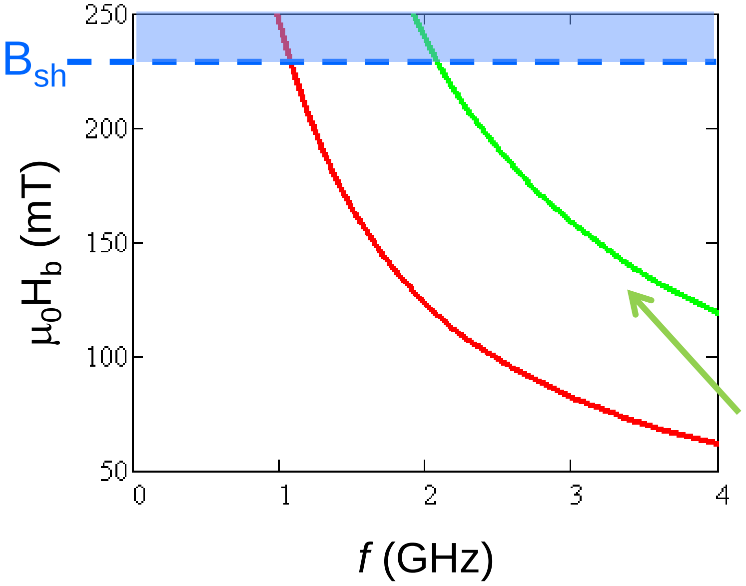

- Higher frequencies not only reduce the cavity Q_0 ($\uparrow R_s$) but also the breakdown field

For 1.5 μm thick Nb on 3 mm thick Copper ($h_{K,Cu}$=8.4 kW/m² K, κ_{Cu}=200 W/m K)

In case of multilayers the thermal conductance is:

$$\alpha = \frac{h_K}{1 + h_K\left[\frac{d}{\kappa} + N\left(\frac{d_i}{\kappa_i} + \frac{d_s}{\kappa_s}\right)\right]}$$

Nb_3Sn coating with Nd_s = 100 nm, $\kappa_s = 10^{-2}$ W/m K
Insulating Al_2O_3 layers, Nd_i = 10 nm, κ_i = 0.3 W/m K
$d_i/\kappa_i = 1/300(d_s/\kappa_s) \rightarrow$ Insulating layers are negligible
$d/\kappa = 3Nd_s/\kappa_s \rightarrow$ TFML adds ~30% to the thermal resistance of the Nb shell

$Q_0(B_0)$ curve

- Because of the $T_m(H_0)$ dependence, R_s acquires a H_0-dependence

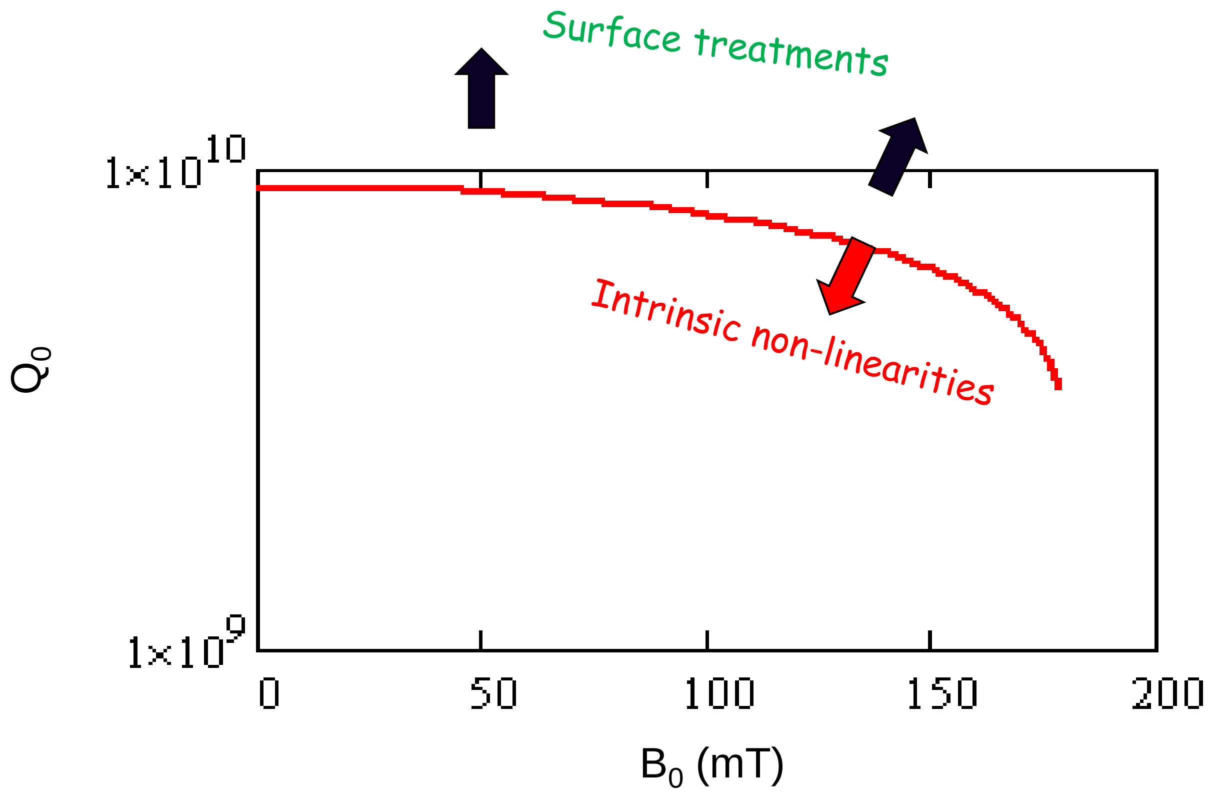

Nb, 2 K, 1.5 GHz,
G=280 Ω, R_s and thermal parameters as in previous slides

SRF applications and cavity requirements

Jefferson Lab

Type of an SRF accelerator	Requirements	RF parameters to pay attention to	Critical elements of the cavity design
Pulsed linacs	• High gradient operation	E_{pk} / E_{acc} H_{pk} / E_{acc}	• Iris & equator shape • Smaller aperture
CW linacs and ERLs	• Low cryogenic losses (dynamic) • Good fill factor	$G \times (R/Q)$ Number of cells per cavity	• Cell shape • Smaller aperture • Larger number of cells
Storage rings and ERLs	• High beam current	$(R/Q)Q_L$ of HOMs	• Larger aperture • Fewer number of cells • Cavity shape
Storage rings, ERL injectors	• High beam power	$P_{coupler}$	• Larger aperture • Fewer number of cells • Single cell cavities for storage rings

Also New Developments for Accelerators for Societal Needs
- See Kazuya Osaki Lecture, Accelerators for medical and industrial applications

The specific application, facility requirements and mode of operation will define the choice of the cavity type, operating frequency, other parameters to optimize.

Design Considerations

Jefferson Lab

- ***Residual resistivity***: $R_{actual} \equiv R_{BCS} + R_{residual}$
- ***Dependence on field*** – shape, material, preparation
  - "Q slope" Electropolishing, baking
  - Field emission- cleanliness, chemical processing
  - Thermal conductivity, thermal breakdown – High RRR
- ***Multipacting*** – cavity shape, cleanliness, processing
- ***Higher Order Modes*** – loss factor, couplers
- ***Mechanical modes***– stiffening, isolation, feedback

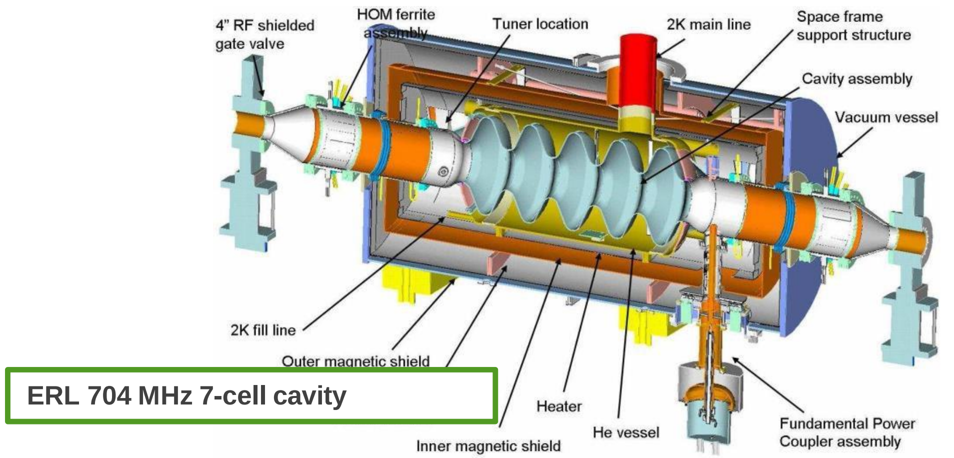

ERL 704 MHz 7-cell cavity

SRF cavity is a complicated electro-mechanical assembly and consist of:
- bare cavity shell with power and HOM couplers
- stiffening elements (ring, bars)
- welded LHe vessel
- Slow and fast frequency tuners
- vacuum ports

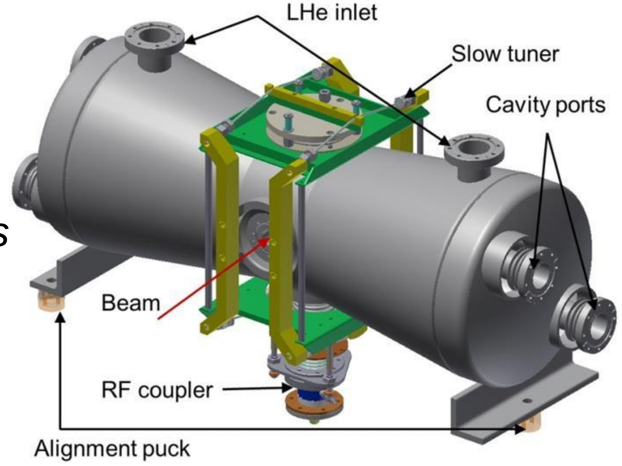

HWR 162.5 MHz cavity for PIP-II

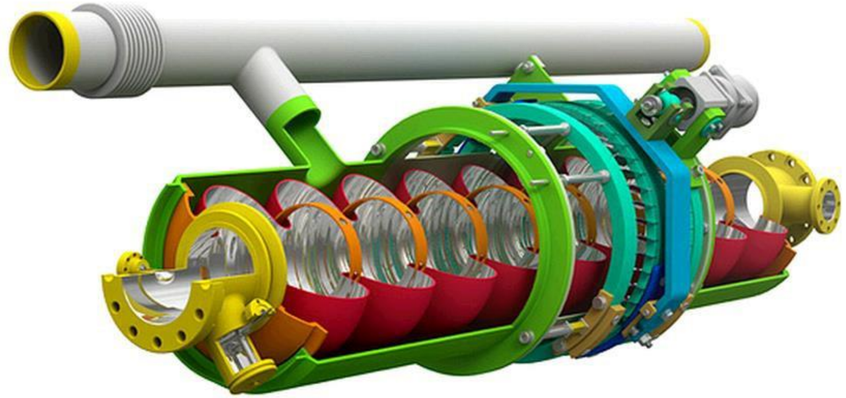

ILC 1.3 GHz 9-cell cavity

The design of SRF cavity requires a complex, self consistent electro-mechanical analysis in order to minimize microphonics and/or Lorentz force detuning phenomena and preserving a good cavity tenability simultaneously !

SRF system design is an intricate process

What shall we consider when designing a cavity?

- ***Material*** (impacts losses and operating gradient)
- ***Frequency*** (impacts size of the cavity, cost, surface resistance, assembly technique, …)
- ***Number of cells*** (impacts field flatness, tunability, HOM extraction, linac fill factor, mechanical resonances, …)
- ***Aperture size*** (impacts beam stability, peak fields, HOM damping, …)
- ***Cavity shape*** (impacts peak surface fields, power dissipation, multipacting, tunability, …)
- …

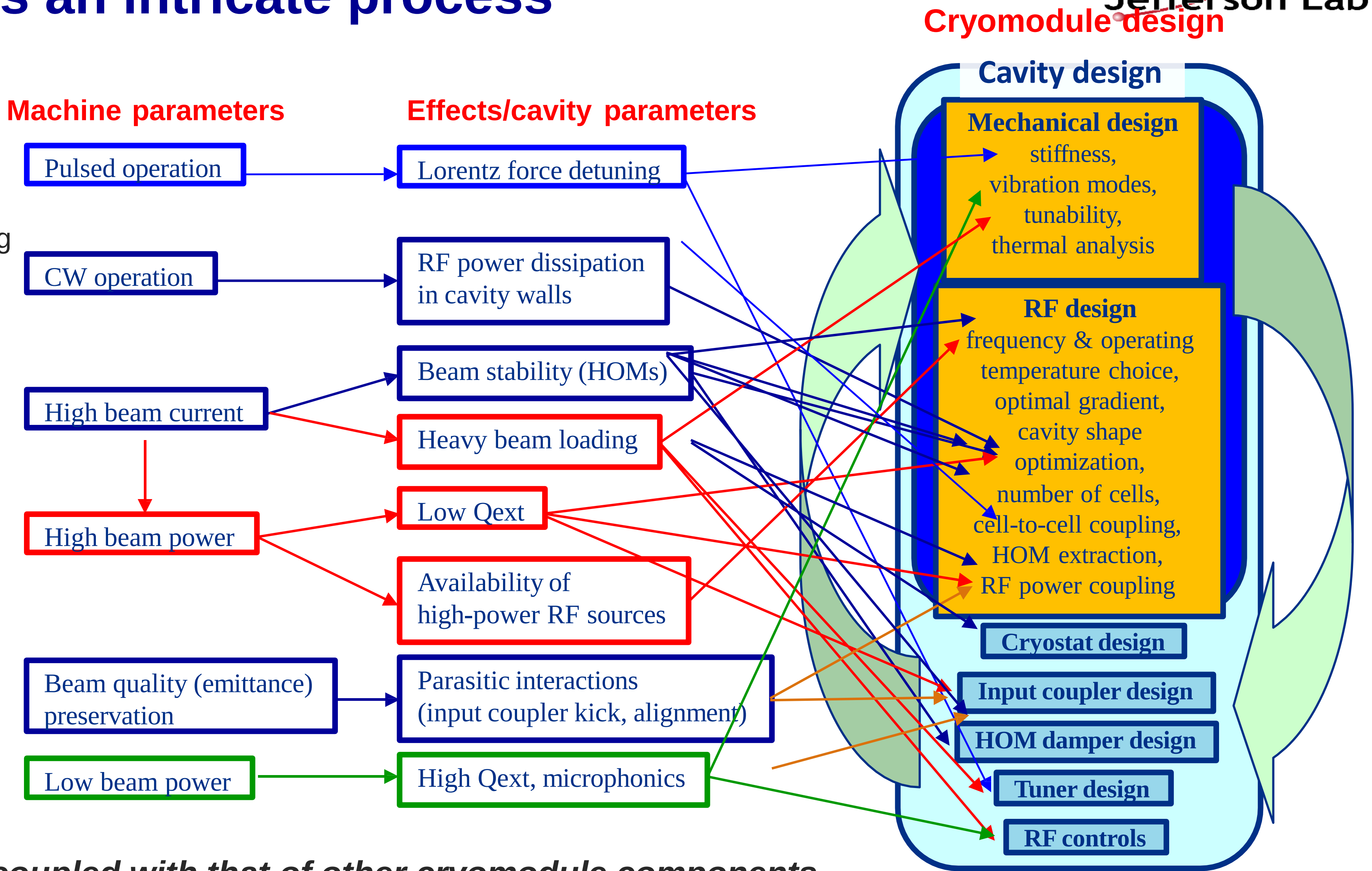

The cavity design is intimately coupled with that of other cryomodule components.

RF simulations tools

As the real cavity cannot be modeled analytically, we use computer codes

1. Electromagnetic field calculations

- Fundamental & High Order Modes spectrum, R/Q, G, fields
  - 2D simulation tools: SUPERFISH, SLANS/CLANS
  - 3D simulation tools: CST Microwave Studio, HFSS, Omega3P, Comsol Multiphysic ANSYS

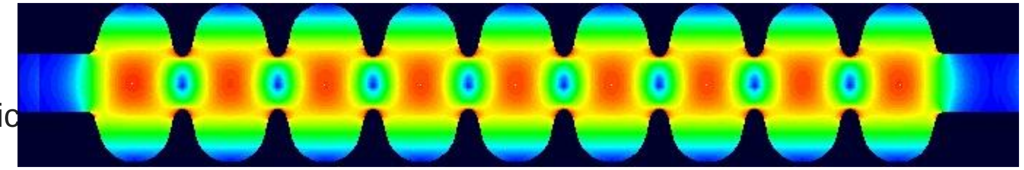

2. Multipacting simulations

- Determine the areas and voltage levels prone to multipacting
  - CST Particle Studio (Particle In Cell, Tracking), SPARK3D, Track3P, MultiPac, MultP-

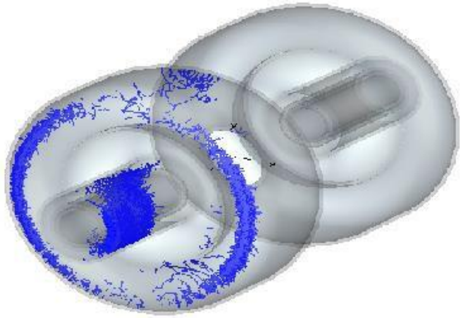

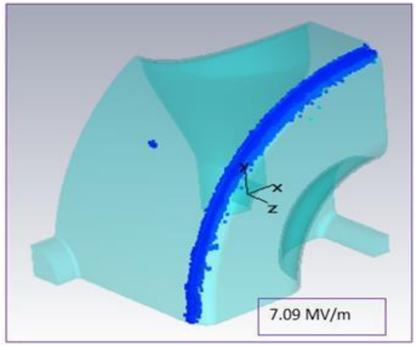

3. Wakefield simulations

- Wake potential, wake impedance
  - CST Microwave Studio, ABCI, ECHO, GdfidL

4. Mechanical simulations

- Mechanical modes and frequencies, thermal deformations, Lorentz force detuning, mechanical stresses
  - ANSYS, Comsol Multiphysics, CST, TEM3P

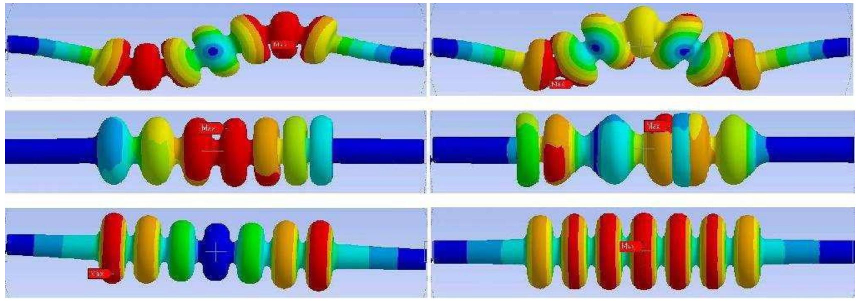

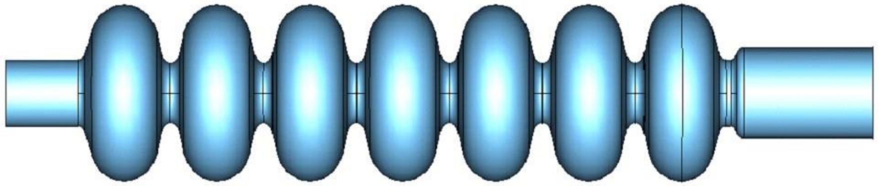

Types of SRF cavities

- There are two distinct types of superconducting RF cavities.
- The first type, ***elliptical* TM-mode cavities**, is for accelerating charged particles that move at nearly the speed of light, such as electrons in high- energy linacs or storage rings.
- The second type, **TEM-mode cavities**, is for particles that have velocities v much smaller than the speed of light c (e.g., β = 0.01…0.5, where $\beta = v/c$), such as the heavy ions or protons at the early stages of acceleration.
- At intermediate velocities, both types of structures could be used, depending on application.

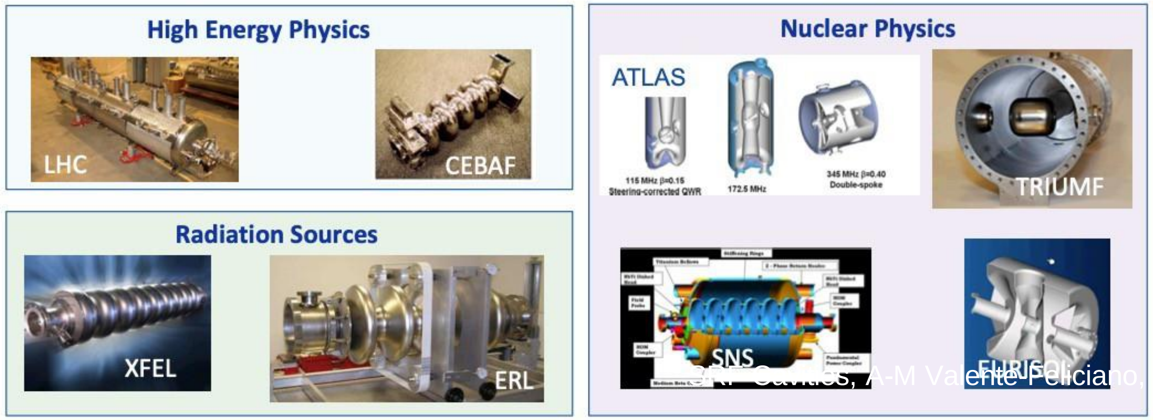

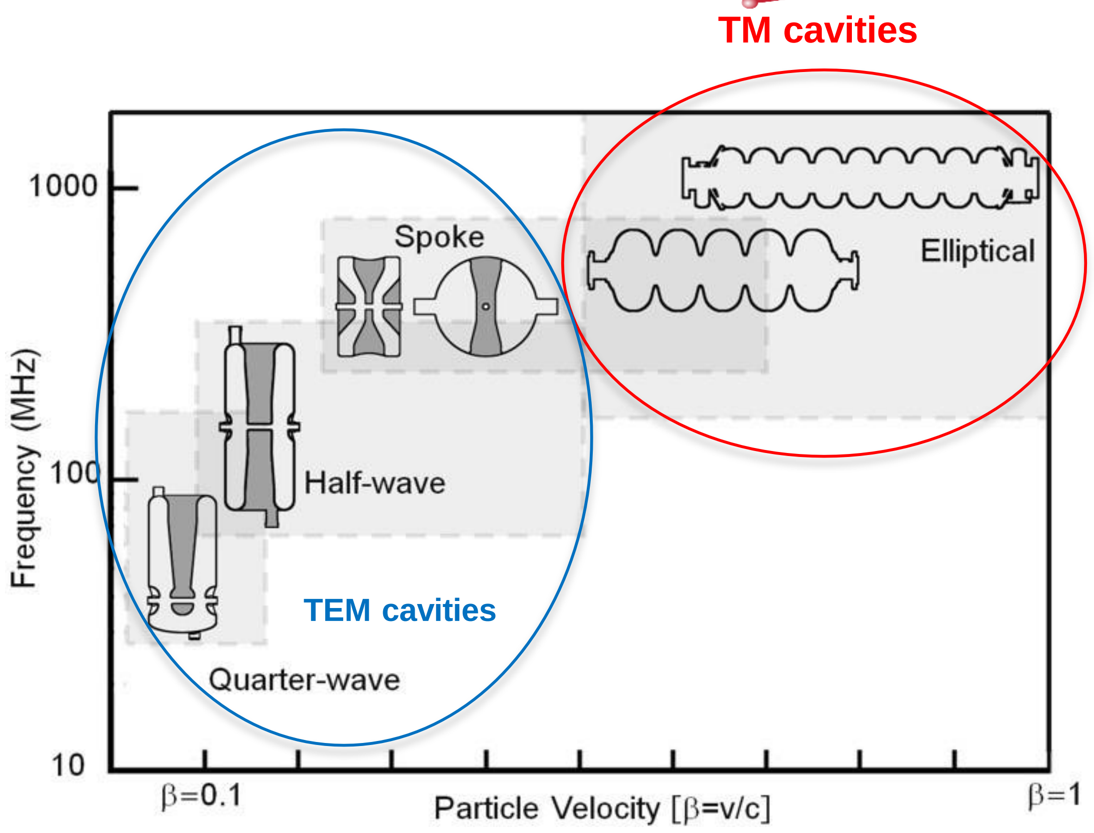

Some practical geometries for different particle velocities

Low β Resonators

Split Loop Resonator

Spoke cavity

Multi-spoke

Quarter Wave Resonator

Elliptical

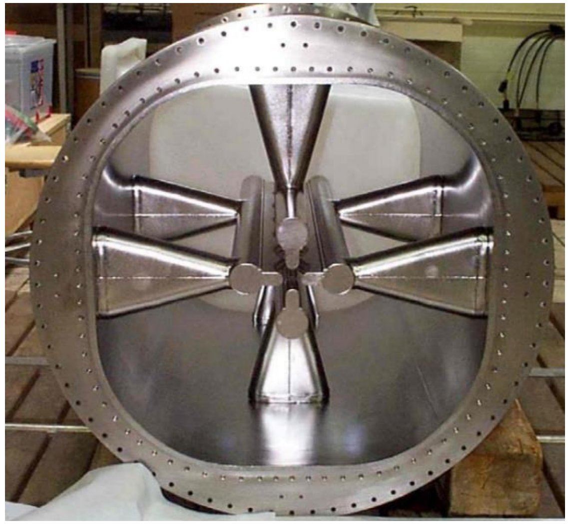

Radio Frequency Quadrupole

Critical applications:
Heavy ion accelerators, e.g. RIA
High power protons, e.g. SNS, Project-X

High acceleration gradient

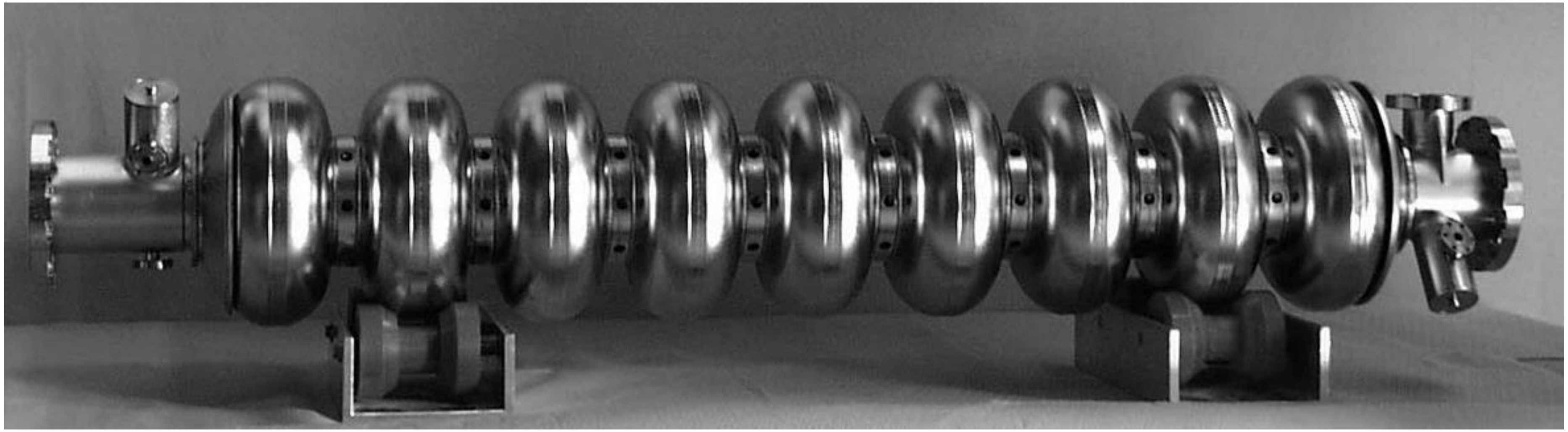

Critical applications:
Linear colliders e.g. ILC
X-ray FELs e.g. DESY XFEL, LCLS-II

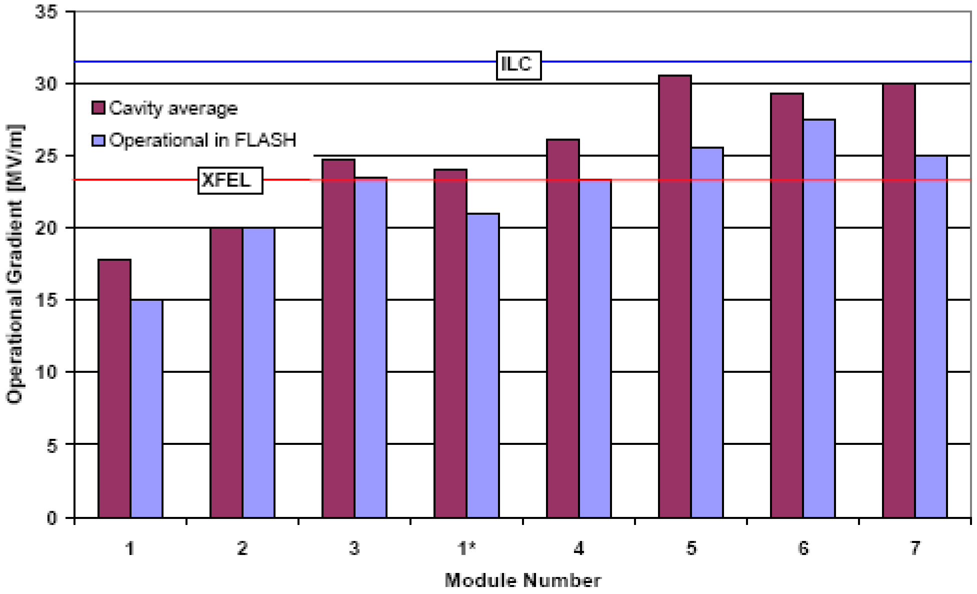

Variety of elliptical cavities

LEP: 352 MHz

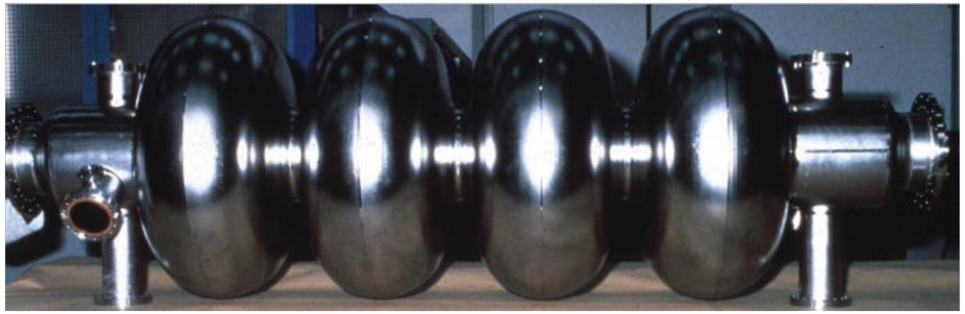

SNS: 805 MHz, β = 0.61 and 0.81

CESR: 500 MHz

KEKB: 508 MHz

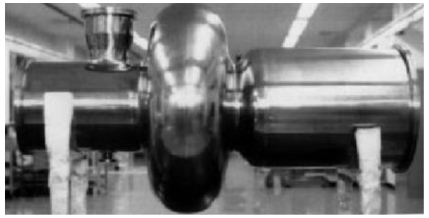

TESLA: 1.3 GHz

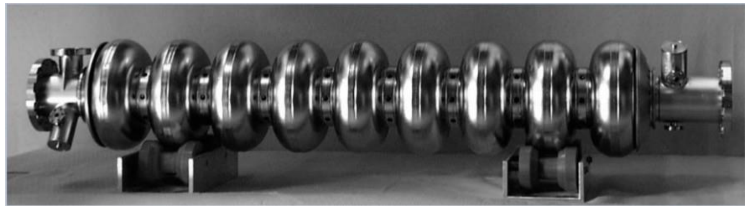

TRISTAN: 508 MHz

CEBAF: 1.5 GHz

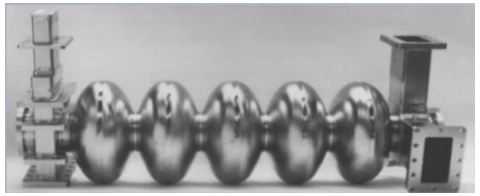

Fermilab: 3.9 GHz

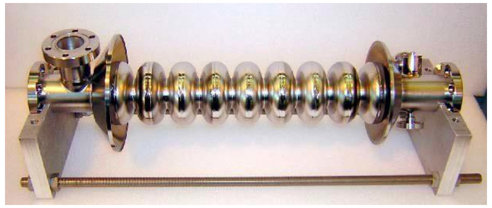

Deflecting Cavities

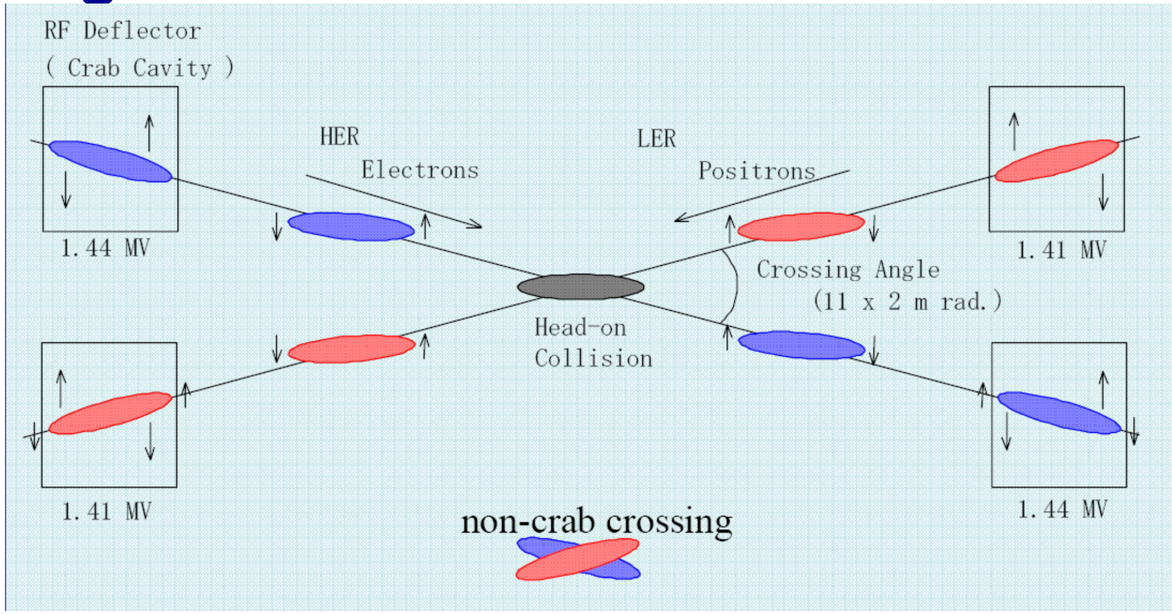

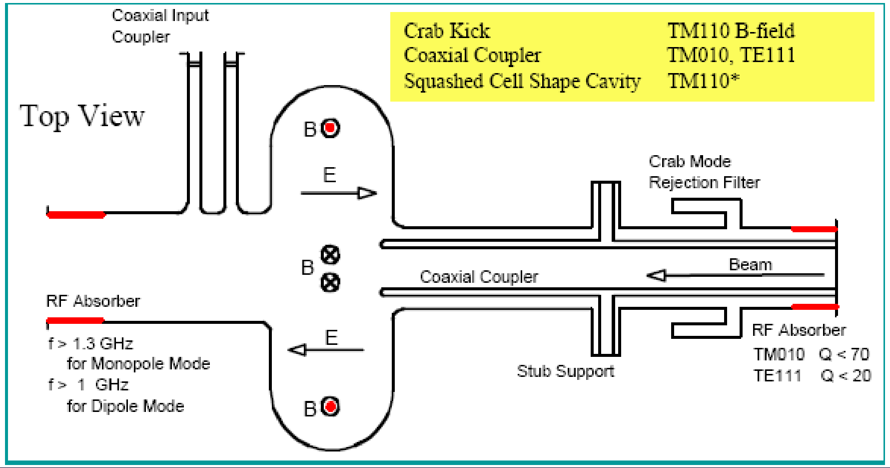

Critical applications:
Crab crossing (luminosity) e.g. KEK-B, LHC
Short X-ray pulses from light sources

High current ERL cavities

- Multi-ampere current possible in ERL

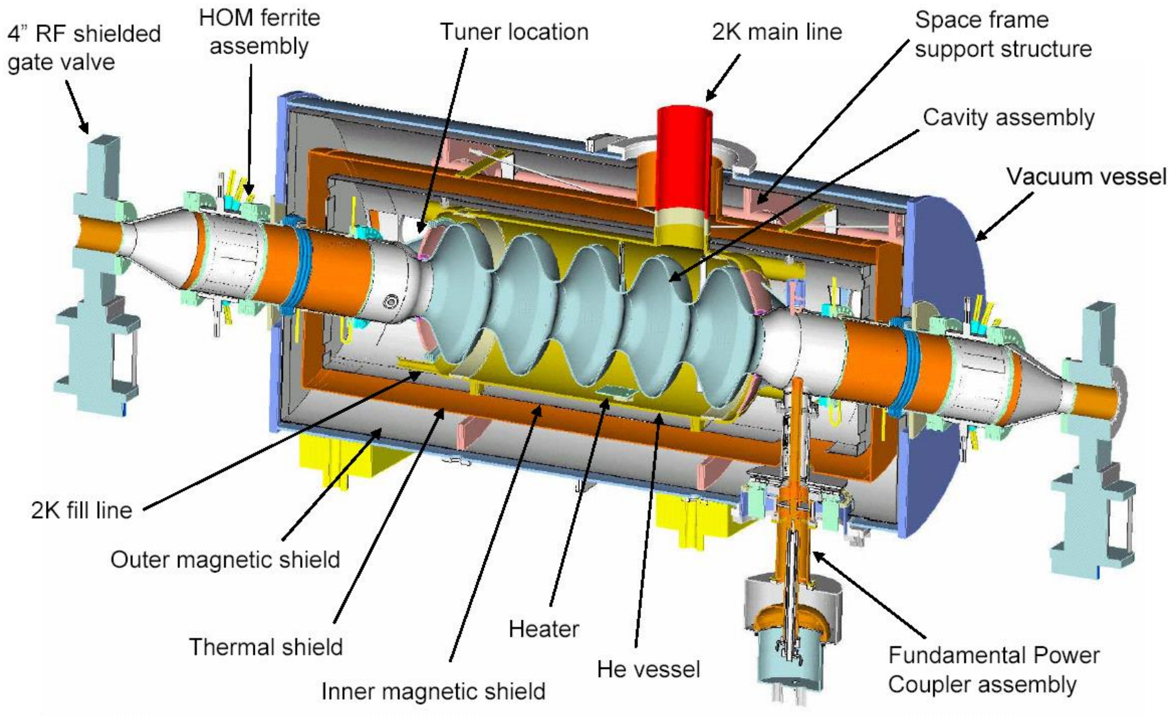

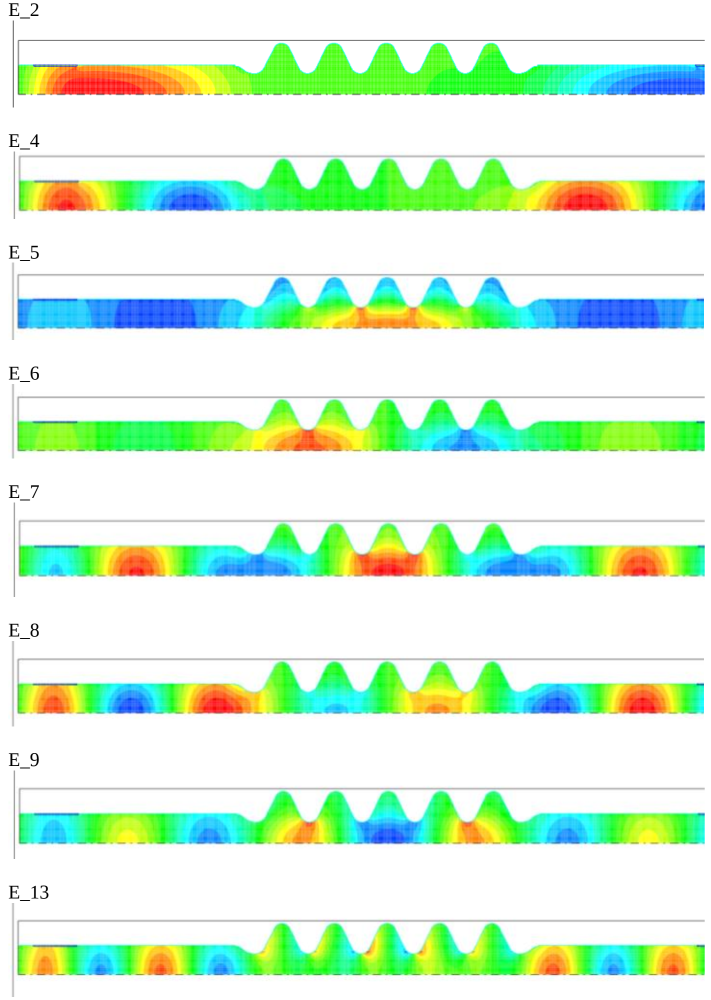

Critical applications:
High average power FELs (e.g. Jlab)
High brightness light sources (e.g. Cornell)
High luminosity e-P colliders (e.g. eRHIC)

High current SRF photo-injector

- Low emittance at high average current is required for FEL.
- The high fields (over 20 MV/m) and large acceleration (2 MV) provide good emittance.
- High current (0.5 ampere) is possible thanks to 1 MW power delivered to the beam.
- Starting point for ERL's beam.

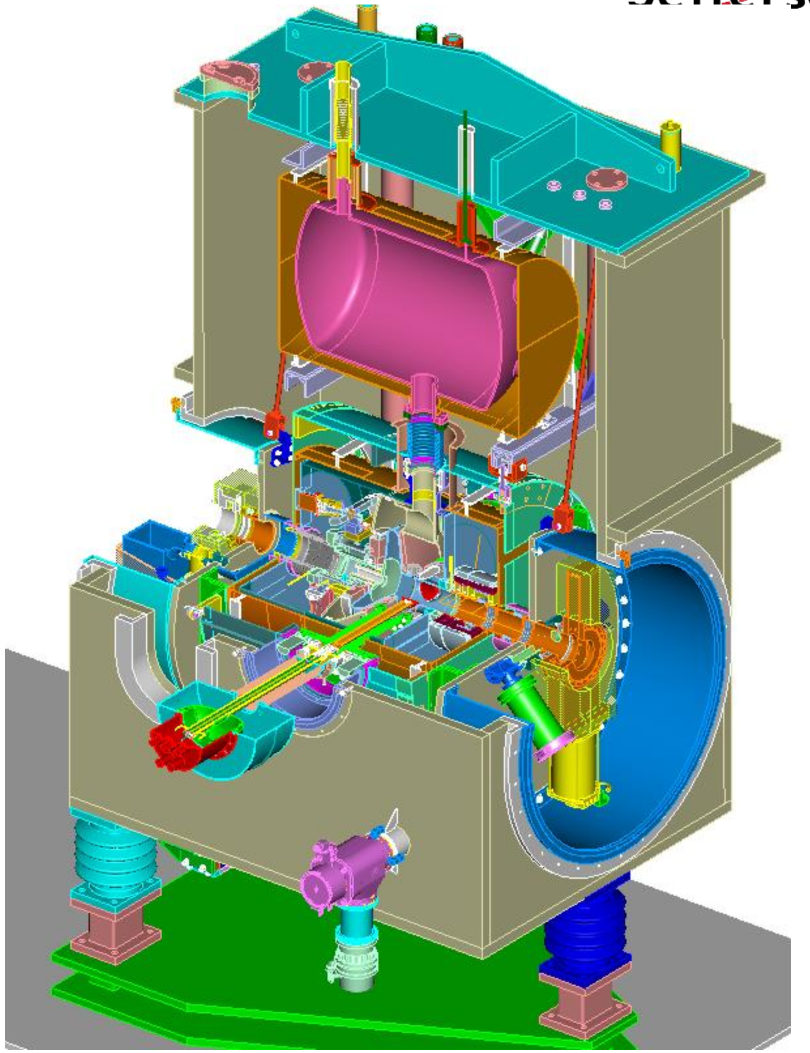

Highlights

- Unlike in the DC case, dissipation occurs in SC in RF because of the inertia of Cooper-pairs
- The surface resistance can be easily understood in terms of a two-fluid model and is due to the interaction of the E-field (decaying from the surface) with thermally excited normal electrons
- $R_s = R_{BCS} + R_{res}$
  - R_{res}:
    - Residual DC magnetic field
    - Normal-conducting precipitates (NbH)
    - …
  - R_{BCS}:
    - Increases quadratically with frequency
    - Decreases exponentially with temperature
    - Has a minimum as a function of material purity
- The maximum theoretical RF field on the surface of a SC is the superheating field ≈ thermodynamic critical field
- Multilayer films may be a practical way to reach H_{sh} in SC with higher T_c than Nb
- Thermal feedback couples R_s at low field to the breakdown field

Highlights

- Elliptical shape cavities are *de facto* standard for TM mode SRF structures for high *β* particle accelerators.
- The cavity shape shall be optimized for new accelerators based on the machine requirements. A plethora of computer simulation tools is available for multi-variable optimization.
- One should pay careful attention to the cavity interfaces with other components of a cryomodule.
- Mechanical aspects of cavity design are very important and should be carefully modeled using appropriate codes.
- High purity bulk Nb (RRR > 250), typically in the form of several mm thick sheets, is used for fabricating the majority of SRF cavities nowadays.
- The fabrication processes are well understood and developed. Some alternative fabrication techniques are being pursued.
- Nb/Cu is used for SRF cavities in several machines, e.g., LEP2, LHC, SOLEIL, HIE-ISOLDE (not covered in this tutorial).
- Nb_3Sn is a promising material, but still in an early R&D stage and demonstrated fields only up to 25 MV/m.

Further Remarks

Jefferson Lab

SRF technology applied to accelerators is wonderfully complex

- ❑ Inherently multi-disciplinary
- ❑ Huge number of coupled parameters – everything matters
- ❑ If you like simplicity – *find other work*
- ❑ Remember that cost-effectiveness drives <u>everything</u>
  - ❑ Research, design, fabrication, processing, maintenance, operation
  - ❑ Nothing is cheap
  - ❑ We only do this because there is no better way to meet the need
- ❑ Designs build upon previous design and operation experience
- ❑ Learn from the insights, successes, and difficulties of others
- ❑ Accumulated physical understanding is required for engaging unexpected problems
- ❑ Contamination can spoil everything.
- ❑ **But when it works right, it makes the amazing possible.**

Basic SRF cavity…

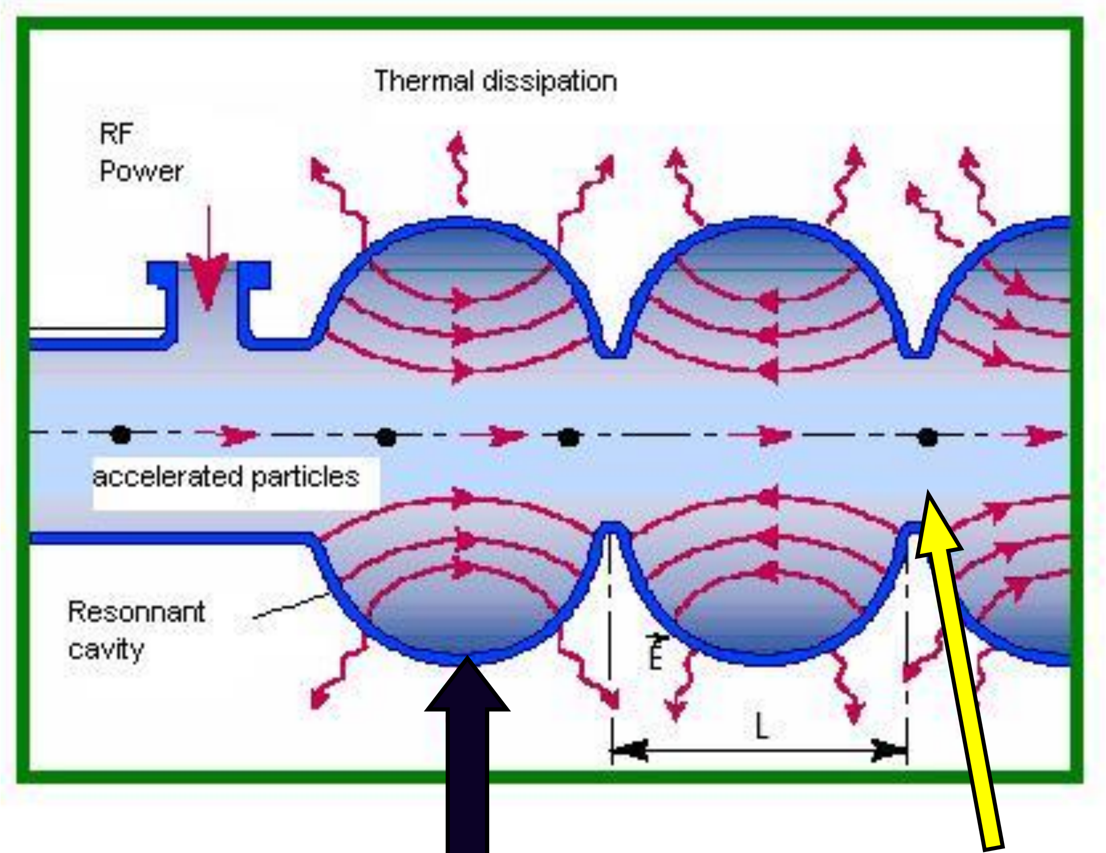

Region of highest magnetic field

Region of highest electric field

Quality factor

$Q_0 \propto G / R_s$

G = geometry factor

i.e. E_{acc} depends on the shape

Surface resistance R_S

R_S(Nb) ~ 1 nΩ @ 2K

<< R_s(Cu) ~ 100 μΩ

E_{surf} ~ 10^6-10^7 V/m

J_{surf} ~ 10^9-10^{10} A/m^2

H_{surf} ~ 100 mT or more

λ_L ~ 50 nm

Acknowledgments

- Inspiration and material from earlier lectures from:

Prof. G. Ciovati, Jlab; Prof. A. Gurevich, ODU; Prof. Steven M. Anlage, UMD; Prof. J. Knobloch, BESSY; Prof. H. Padamsee, Cornell U.; S. Belomestnykh, FNAL.

- **Tutorials** on SRF can be found on the webpages of SRF Conferences: http://accelconf.web.cern.ch/accelconf/

References

- Standard textbooks on SRF
  - H. Padamsee, J. Knobloch and T. Hays, *RF Superconductivity for Accelerators*, J. Wiley & Sons, New York, 1998
  - H. Padamsee et al "RF superconductivity for accelerators", 2nd edition, WILEY-VCH (2008)
  - H. Padamsee, *RF Superconductivity. Science, Technology, and Applications*, Wiley-VCH, Weinheim, 2009
- Reviews on SRF
  - J. P. Turneaure et al "The surface impedance of superconductors and normal conductors: the Mattis-Bardeen theory", J. Supercond. 4, 341-355 (1991)
  - A. Gurevich "Theory of RF superconductivity for resonant cavities", Supercond. Sci. Technol. 30 034004 (2017)
  - CERN Accelerator School – 1955 – 2016 (https://cds.cern.ch/collection/CERN%20Yellow%20Reports?ln=en)
- Introduction to solid state physics (before second quantization)
  - N. W. Ashcroft and N. D. Mermin, "Solid State Physics" Thomson Learning (1976)
- Introduction to superconductivity + minimal knowledge on condensed matter physics (but lack of SRF…)
  - S. Fujita and S. Godoy "Quantum statistical theory of superconductivity", Springer, (1996)
- Dictionary of superconductivity
  - M. Tinkham "Introduction to superconductivity", 2nd edition, Dover (2004)
- More advanced textbook on superconductivity
  - N. Kopnin "Theory of Nonequilibrium Superconductivity", Oxford Science Publications (2001)

References

- BCS resistance

  - J. Bardeen, L. N. Cooper, and J. R. Schrieffer,Phys. Rev.108, 1175 (1957). [Matrix elements for static magnetic field were calculated here]
  - D. C. Mattis and J. Bardeen, Phys. Rev.111,412 (1958). [1st order perturbation of RF response and nonlocality, substituting matrix elements modified for RF]
  - J. Halbritter, Z. Physik266, 209 (1974) [Fermi's golden rule applied for constant martix element and two fluid *approximation*]
  - J. Halbritter, KFK-Ext.03/70-06 (1970) [FORTRAN66 code for BCS resistance of f<τ1/2 and arbitrary ξ_0, λ_L, l]

- Residual resistance due to flux oscillation

  - J. Bardeen and M. J. Stephen, Phys. Rev.140, A1197(1965). [Phenomenological model to describe trapped flux as a string]
  - J. I. Gittleman and B. Rosenblum, Phys. Rev. Lett.16,734 (1966). [driven-damped ordinary differential equation for flux oscillation driven by Lorentz force]
  - M. Checchin, M. Martinello, A. Grassellino, A. Roma-nenko, and J. F. Zasadzinski, Supercond. Sci. Technol.30, 3 (2017). [application of Gittleman & Rosenblum for SRF cavities]
  - A. Gurevich and G. Ciovati, Phys. Rev. B87, 054502 (2013). [keeping tension term and solved partial differential equation instead]

- Quench field

  - J. Matricon and D. Saint-James Phys Lett A 24 241 (1967). [solving Ginzburg-Landau equation to estimate superheating field]
  - F. P.-J. Lin and A. Gurevich, Phys. Rev. B 85, 054513 (2012). [solving Eilenberger equations to estimate superheating field in arbitrary impurity]
  - Vudtiwat Ngampruetikorn and J. A. Sauls, Phys. Rev. Research 1, 012015(R) (2019). [including inhomogeneity at the surface]

BACK-UPS

Figures of Merit

Accelerating voltage and transit time

For efficient acceleration, choose a cavity geometry and a mode where:

- Electric field is along the particle trajectory
- Magnetic field is zero along the particle trajectory
- Velocity of the electromagnetic field is matched to particle velocity

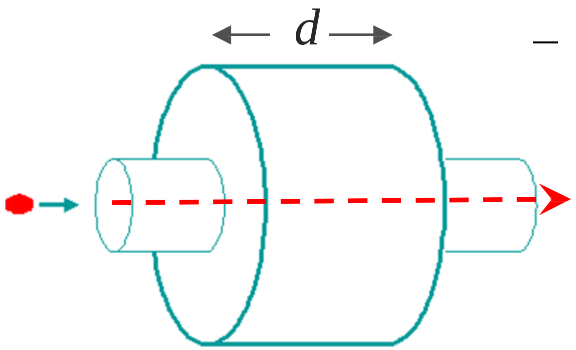

- Assuming charged particles moving along the cavity axis, one can calculate accelerating voltage as $V_c = \left| \int_{-\infty}^{\infty} E_z(\rho = 0, z) e^{i\omega_0 z/\beta c} dz \right|$

For the pillbox cavity we can integrate this analytically: $V_c = E_0 \left| \int_0^d e^{i\omega_0 z/\beta c} dz \right| = E_0 d \frac{\sin\left(\frac{\omega_0 d}{2\beta c}\right)}{\frac{\omega_0 d}{2\beta c}} = E_0 d \cdot T$

where T is the transit time factor.

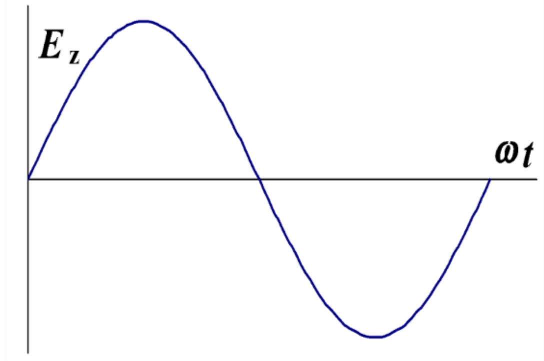

- To get maximum acceleration:

$$T_{(,-./\&(} = t_{01\&(} - t_{0.(0,} = \frac{T_*}{2} \Rightarrow d = \frac{\beta\lambda}{2} \Rightarrow V_! = \frac{2}{\pi} E_* d$$

Thus, for the pillbox cavity $T = 2/\nu$.

Accelerating Gradient (E_{acc})

- Accelerating field (gradient) is defined as the voltage gained by a particle divided by a reference length

$$E_{acc} = \frac{V_c}{d}$$

- For velocity of light particles:

  N – no. of cells

$$d = \frac{N\lambda}{2}$$

- For less-than-velocity-of-light cavities ($\beta < 1$), there is no universally adopted definition of the reference length
- However multi-cell elliptical cavities with $\beta < 1$ Length per cell $d = \frac{\beta\lambda}{2}$

Unfortunately, the cavity length is not easy to specify for shapes other than pillbox so usually it is assumed to be ***d = βλ/2****. This works OK for multi-cell cavities, but poorly for single-cell cavities or low β cavities*

Stored energy & quality factor

- Energy density in electromagnetic field:

$$u = \frac{1}{2}\left(\varepsilon_0 \mathbf{E}^2 + \mu_0 \mathbf{H}^2\right)$$

Measures cavity performance as to how lossy cavity material is for given stored energy

- Because of the sinusoidal time dependence and $90°$ phase shift, the energy oscillates back and forth between the electric and magnetic field. Then the total stored energy in a cavity is given by

$$U = \frac{\varepsilon_0}{2}\int_V dV\,|\mathbf{E}|^2 = \frac{\mu_0}{2}\int_V dV\,|\mathbf{H}|^2$$

- An important **figure of merit** is the ***quality factor***, which for any resonant system is

$$Q_0 \equiv \frac{\text{Energy stored in cavity}}{\text{Energy dissipated in cavity walls per radian}} = \frac{\omega_0 U}{P_{diss}}$$

$$= \omega_0 \tau_0 = \frac{\omega_0}{\Delta\omega_0}$$

$$Q_0 = \frac{\omega\mu_0}{R_s}\frac{\int_V dV\,|\mathbf{H}|^2}{\int_A da\,|\mathbf{H}_{\|}|^2}$$

We are assuming that the surface resistance R_s does not vary over the cavity surface and has no field dependence.

or roughly 2π times the number of RF cycles it takes to dissipate the energy stored in the cavity. It is determined by both the material properties and cavity geometry and is ~10^4 for NC cavities and ~10^{10} for SC cavities at 2 K.

Recall that the surface resistance is the internal resistance for a unit length and unit width and for NC materials is $R_/ = \frac{4}{\text{OP}}$,
where σ is the material conductivity and δ is the skin depth.

Peak surface fields

$$E_{pk} = E_0 J_0(0) = E_0 = \frac{\pi}{2} E_{acc} = 1.57\, E_{acc}$$

$$H_{pk} = \frac{E_0}{\eta} J_1(1.841) = \frac{\pi}{2} \frac{E_{acc}}{\eta} J_1(1.841)$$

$$\frac{H_{pk}}{E_{acc}} = 2430\, \frac{\text{A/m}}{\text{MV/m}} = 30.5\, \frac{\text{Oe}}{\text{MV/m}}$$

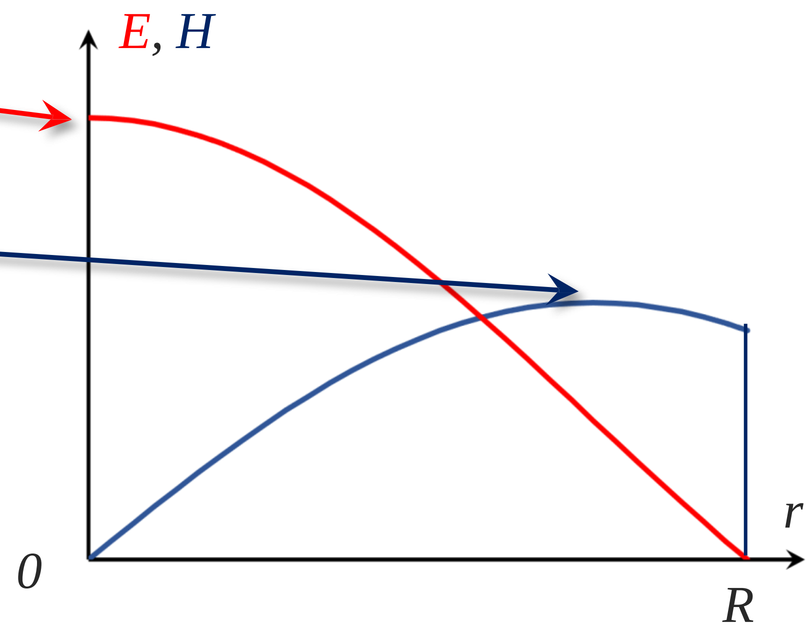

- Peak surface fields are important for the SRF cavity performance. They should be made as small as possible in ”real” cavities. Pillbox will serve as a reference.
- The peak surface electric field is responsible for field emission.
- The peak surface magnetic field has fundamental limit: critical field of SC state.

Power Dissipation (P_{diss})

- Surface current results in power dissipation proportional to the surface resistance (R_s)
- Power dissipation per unit area $\frac{dP}{da} = \frac{\mu_0 \omega \delta}{4} |\mathbf{H}_{\parallel}|^2 = \frac{R_s}{2} |\mathbf{H}_{\parallel}|^2$
- Total power dissipation in the cavity walls $P = \frac{R_s}{2} \int_A da |\mathbf{H}_{\parallel}|^2$

To minimize the losses, one needs to maximize the denominator. By modifying the formula, one can make the denominator material-independent: $G \cdot R/Q$ – this new parameter depends only on the cavity geometry and can be used during cavity shape optimization.

Frequency dependence

$$\frac{P}{L} \propto \frac{1}{\frac{R}{Q} Q R_S} \frac{E^2 R_S}{\omega}$$

- For normal conductors → $R_S \propto \omega^{1/2}$
  - per unit length $\frac{P}{L} \propto \omega^{-\frac{1}{2}}$
  - per unit area $\frac{P}{A} \propto \omega^{\frac{1}{2}}$
- For superconductors → $R_S \propto \omega^2$
  - per unit length $\frac{P}{L} \propto \omega$
  - per unit area $\frac{P}{A} \propto \omega^2$

- NC cavities favor high frequencies, ***SC cavities favor low frequencies.***

Geometrical Factor (G)

- Geometrical factor [Ω]
  - Product of the qualify factor (Q_0) and the surface resistance (R_s)

$$G = QR_s = \omega\mu_0 \frac{\int_V dV\,|\mathbf{H}|^2}{\int_A da\,|\mathbf{H}_{\parallel}|^2} = 2\pi\sqrt{\frac{\mu_0}{\varepsilon_0}}\frac{1}{\lambda}\frac{\int_V dV\,|\mathbf{H}|^2}{\int_A da\,|\mathbf{H}_{\parallel}|^2} = \frac{2\pi\eta}{\lambda}\frac{\int_V dV\,|\mathbf{H}|^2}{\int_A da\,|\mathbf{H}_{\parallel}|^2}$$

  - Independent of size and material

$\eta \approx 377\Omega$ Impedance of vacuum

  - Depends only on shape of cavity and electromagnetic mode

very useful for comparing different cavity shapes.

For the pillbox cavity we get $G = 257\ \Omega$. If the cavity is made of copper ($\sigma = 5.8\times10^7$ S/m) and operates at 1.5 GHz, we get $\delta = 1.7\ \mu$m, $R_s = 10\ \text{m}\Omega$, and $Q_0 = G/R_s = 25{,}700$

Shunt Impedance (R_{sh}) and R/Q

- Shunt impedance (R_{sh}) [Ω] characterizers losses in a cavity $$R_{sh} \equiv \frac{V_c^2}{P_{diss}}$$
- Maximize shunt impedance to get maximum acceleration
- Note: Sometimes the shunt impedance is defined as or quoted as impedance per unit length (Ω/m) $$\frac{V_c^2}{2P_{diss}}$$

A related quantity is the ratio of the shunt impedance to the quality factor, which is independent of the surface resistivity and the cavity size:

- R/Q [Ω]: Measures of how much of acceleration for a given power dissipation

  *This parameter is frequently used as a figure of merit and is useful in determining the level of mode excitation by bunches of charged particles passing through the cavity. Sometimes it is called the **geometric shunt impedance**.* *For the pillbox cavity R/Q = 196 Ω*

$$\frac{R}{Q} = \frac{V^2}{P}\frac{P}{\omega U} = \frac{E^2}{U}\frac{L^2}{\omega}$$

- Optimization parameter: $$R_{sh}R_s = \frac{R_{sh}}{Q}QR_s = \frac{R}{Q}G$$

  R/Q and $R_{sh}R_s$
  - Independent of size (frequency) and material
  - Depends on mode geometry
  - Proportional to no. of cells

In practice for elliptical cavities
- $R/Q \sim 100$ Ω per cell
- $R_{sh}R_s \sim 33{,}000\ \Omega^2$ per cell

TM_{010} Mode in a Pill Box Cavity

Energy content

$$U = \varepsilon_0 E_0^2 \frac{\pi}{2} J_1^2(x_{01}) L R^2$$

Power dissipation

$$P = E_0^2 \frac{R_s}{\eta^2} \pi J_1^2(x_{01})(R+L)R$$

$$x_{01} = 2.40483$$

$$J_1(x_{01}) = 0.51915$$

Geometrical factor

$$G = \eta \frac{x_{01}}{2} \frac{L}{(R+L)}$$

Energy Gain

$$\Delta W = E_0 \frac{\lambda}{\pi} \sin\frac{\pi L}{\lambda}$$

Gradient

$$E_{acc} = \frac{\Delta W}{\lambda/2} = E_0 \frac{2}{\pi} \sin\frac{\pi L}{\lambda}$$

Shunt impedance

$$R_{sh} = \frac{\eta^2}{R_s} \frac{1}{\pi^3 J_1^2(x_{01})} \frac{\lambda^2}{R(R+L)} \sin^2\left(\frac{\pi L}{\lambda}\right)$$

Types of SRF cavities

Cavity families (low-β , middle-β & high-β)

TEM$_{001}$ modes in a quarter-wave or half-wave cavity

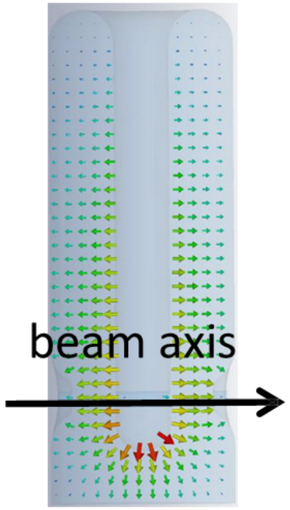

- p+ upstream (<1GeV)
- Heavy ion

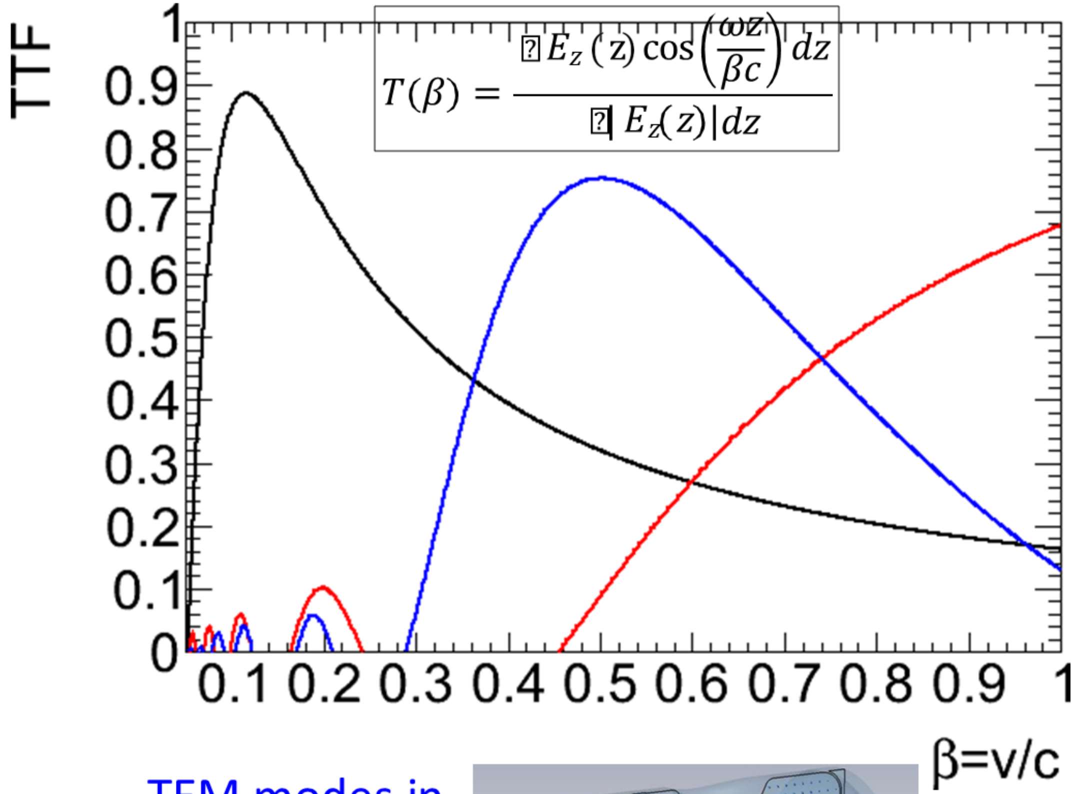

TEM modes in a spoke cavity

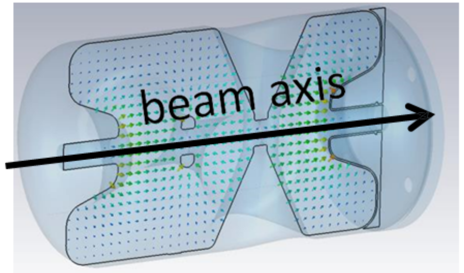

- p+ (<1GeV)

TM$_{010}$ modes in an elliptical cavity

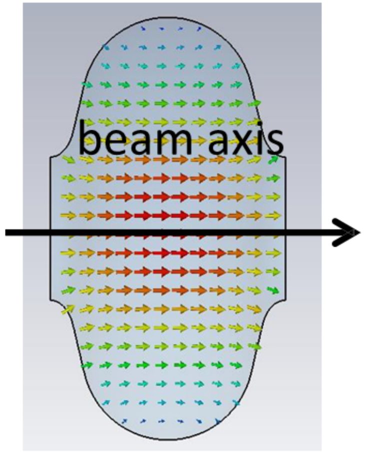

- p+ downstream (>1GeV)
- e-, e+ (>0.5MeV)

SRF Cavity Limitations

Real Performance - Q vs. accelerating field

Jefferson Lab

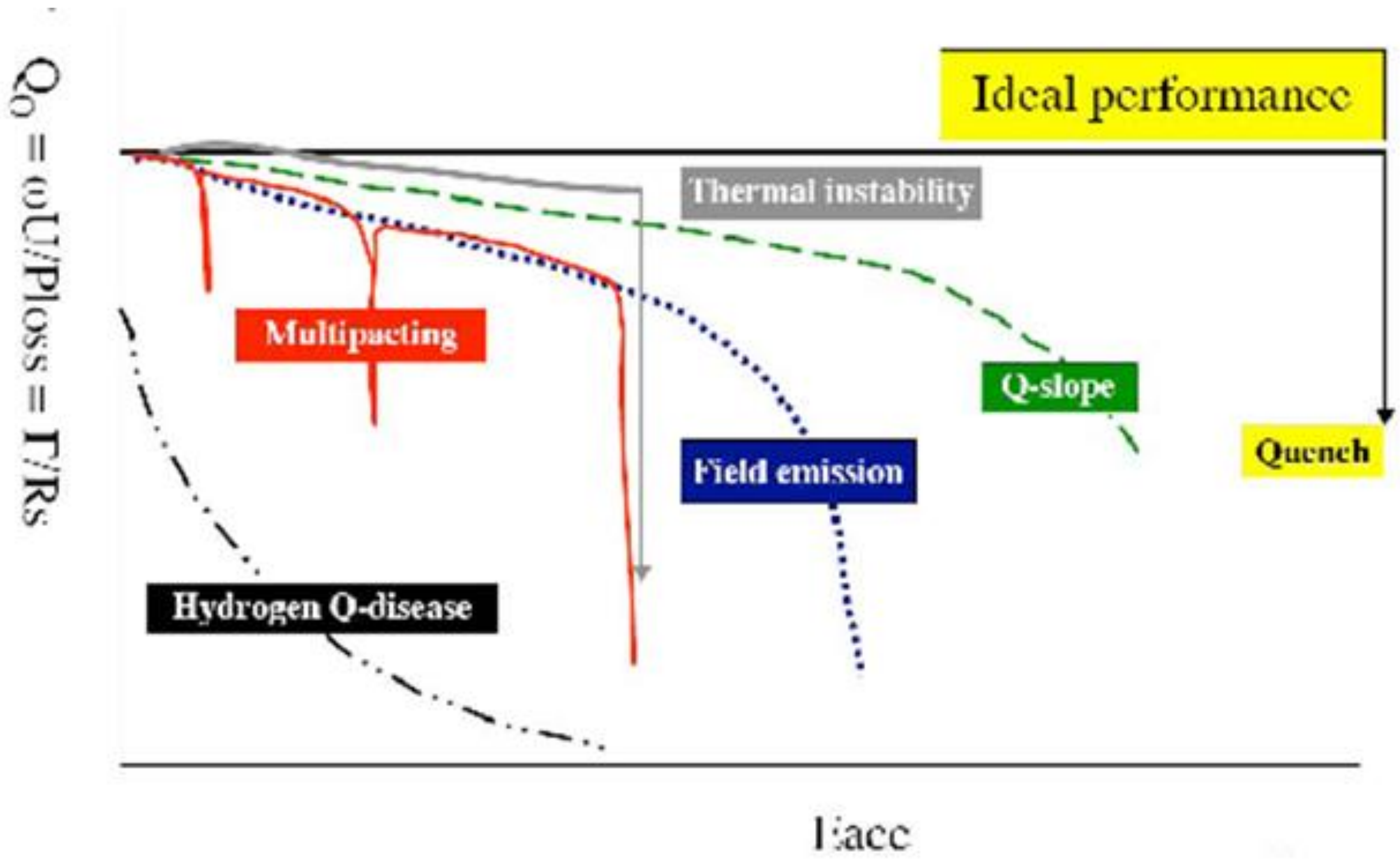

Can be achieved, and recently 2.09 kGauss achieved at Cornell.

Limit on Fields

- Field emission – clean assembly
- Magnetic field breakdown (ultimate limit) - good welds, reduce surface fields
- Thermal conductivity – high RRR material
- Local heating due to defects

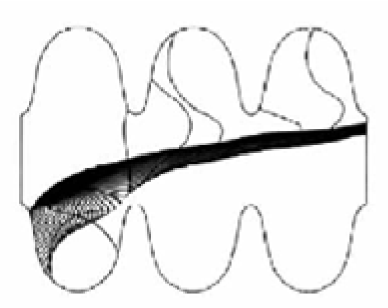

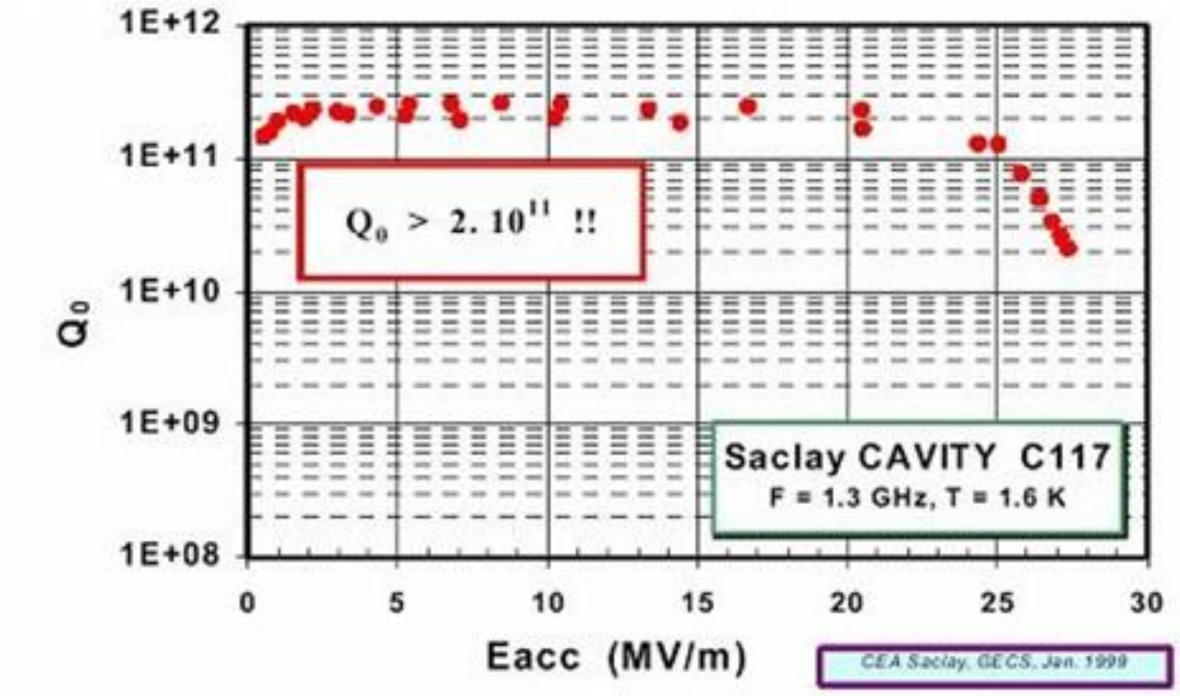

Fields of 20 to 25 MV/m at Q of over 10^{10} is routine

Choice of material and preparation

- High “RRR” material (300 and above)
- Large grain material is an old “new” approach
- Buffered Chemical Polishing (BCP) (HF – HNO_3 – H_2PO_4 , say 1:1:2)
- Electropolishing (HF – H_2SO_4)
- UHV baking (~800 ºC)
- Low temperature (~120 ºC).
- High pressure rinsing
- Clean room assembly

Multipacting

- Multipacting is a resonant, low field conduction in vacuum due to secondary emission
- Easily avoided in elliptical cavities with clean surfaces
- May show up in couplers!

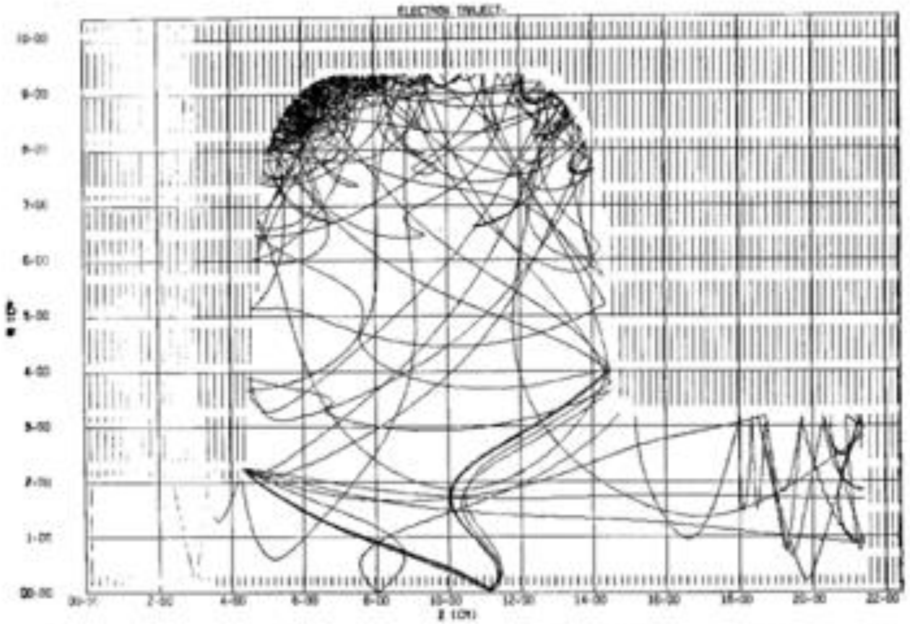

Fig. 6. A typical computer plot of the trajectories in z-r space of ten initial electrons and their second and higher generation electrons produced by the electron multiplication simulation program.

Multipacting in Stanford SCA cavity, 1973 PAC

Higher Order Modes (HOM)

- Energy is transferred from beam to cavity modes
- The power can be very high and must be dumped safely
- Transverse modes can cause beam breakup

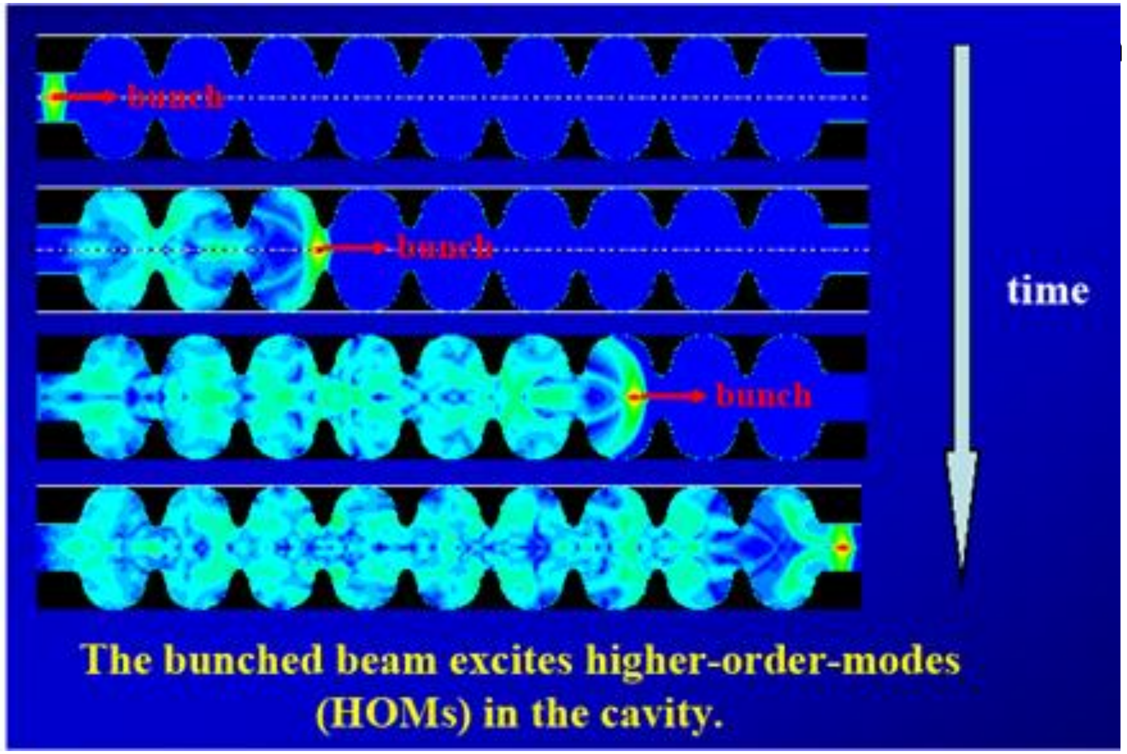

Energy lost by charge q to cavity modes:

$$\Delta U = kq^2$$

Longitudinal
and Transverse

Solution: Strong damping of all HOM,
Remove power from all HOM to loads
Isolated from liquid helium environment.

Electromechanical issues

- Lorentz detuning
- Pondermotive instabilities
- Pressure and acoustic noise

Solutions include

  - broadening resonance curve
  - feedback control
  - good mechanical design of cavity and cryostat

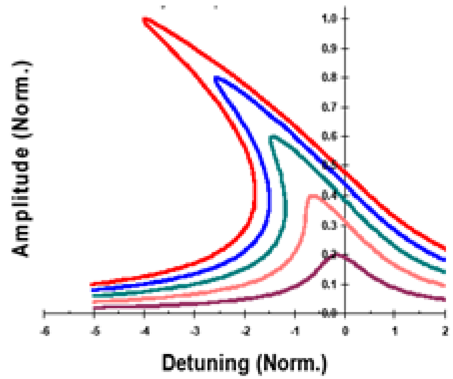

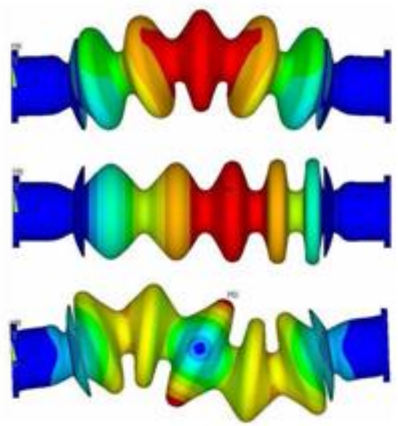

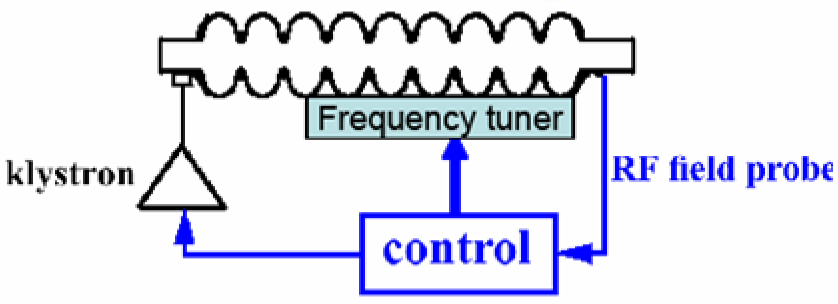

Miscellaneous hardware

- Fundamental mode couplers
- Pick-up couplers
- Higher-Order Mode couplers
- Cryostats (including magnetic shields, thermal shields)
- Helium refrigerators (1 watt at 2 K is ~900 watt from plug)
- RF power amplifiers (very large for non energy recovered elements

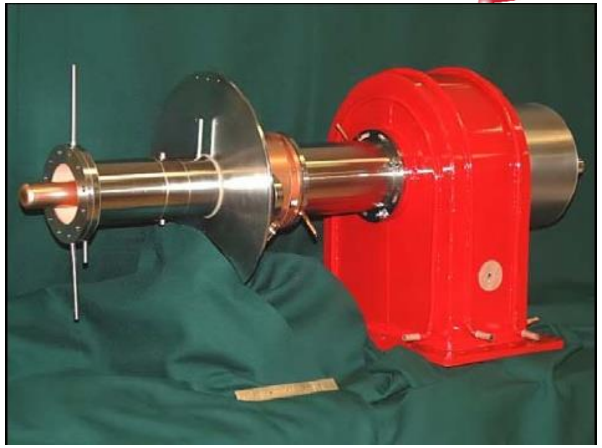

Cavity Fabrication & Preparation

Fabrication and surface preparation steps

Jefferson Lab

- Typical superconducting RF cavities are made of high purity niobium, either in a bulk form or as a thin layer deposited on the inner surface of copper structure.
- To achieve good performance, the high purity of niobium must be maintained throughout the fabrication process.
- In addition, the inner surface of the cavity, exposed to strong electromagnetic fields, must be carefully prepared.

- The bulk niobium cavities are fabricated by electron beam welding of formed or machined parts.
- Typical fabrication and surface processing steps include:
  - Surface inspection and cutting niobium sheets of high RRR material.
  - Forming half-cells by deep drawing, spinning or hydroforming.
  - Forming or machining other parts of the structure: beam pipes, various ports, parts for HOM couplers, etc.
  - Mechanical polishing imperfections and dipping in an HCl or H_2SO_4 bath to eliminate metal impurities; rust checking by dipping overnight in a water bath.
  - Light chemical etching
  - Electron beam welding sub-assemblies.
  - RF testing and tuning of sub-assemblies.
  - Mechanical trimming sub-assemblies as necessary.
  - Light chemical etching
  - Electron beam welding the complete structure from sub-assemblies.
  - Cavity inspection, grinding off imperfections on the inner welding seams, where impurities or micro-cracks might be apparent.
  - Heavy chemical etching (BCP or EP) to remove the mechanically damaged surface layer and other imperfections.
  - High-temperature hydrogen degassing in an all-metal vacuum furnace in a temperature range between 600 and 950°C
  - RF measurements of the cavity frequency. Tuning of the structure to achieve the desired field flatness.
  - Final surface preparation (e.g., nitrogen doping, light EP and HPR) before acceptance testing in a vertical dewar.

Material inspection

- The material must be fully recrystallized, otherwise mechanical properties are affected. Sheet metal forming is sensitive to mechanical properties. In particular, a uniform grain size is essential.
- Nb sheets are inspected upon receiving, visually and using eddy-current or SQUID scanning (more sensitive). The basic principle is to detect the alteration of the eddy currents with a double coil sensing probe to identify inclusions and defects embedded under the surface.
- Usually, a very small fraction of sheets is rejected at this stage.

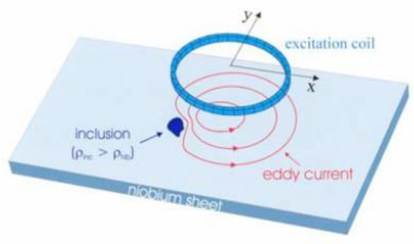

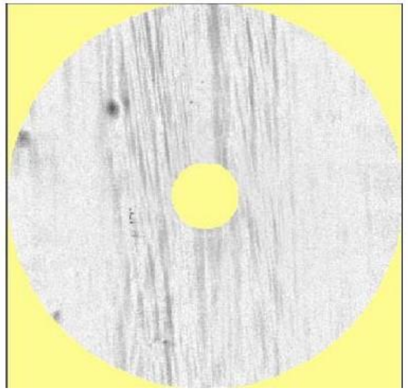

Technical Specification to Niobium Sheets for XFEL Cavities

Concentration of impurities in ppm				Mechanical properties	
Ta	≤ 500	H	≤ 2	RRR	≥ 300
W	≤ 70	N	≤ 10	Grain size	≈ 50 µm
Ti	≤ 50	O	≤ 10	Yield strength, $\sigma_{0.2}$	$50 < \sigma_{0,2} < 100$ N/mm² (MPa)
Fe	≤ 30	C	≤ 10	Tensile strength	> 100 N/mm² (Mpa)
Mo	≤ 50			Elongation at break	30 %
Ni	≤ 30			Vickers hardness HV 10	≤ 60

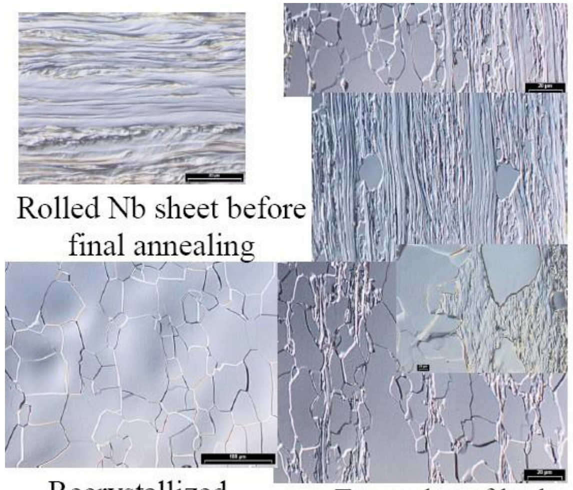
Rolled Nb sheet before final annealing
Recrystallized niobium sheet
Examples of bad recrystallization

Overview of cavity fabrication flow

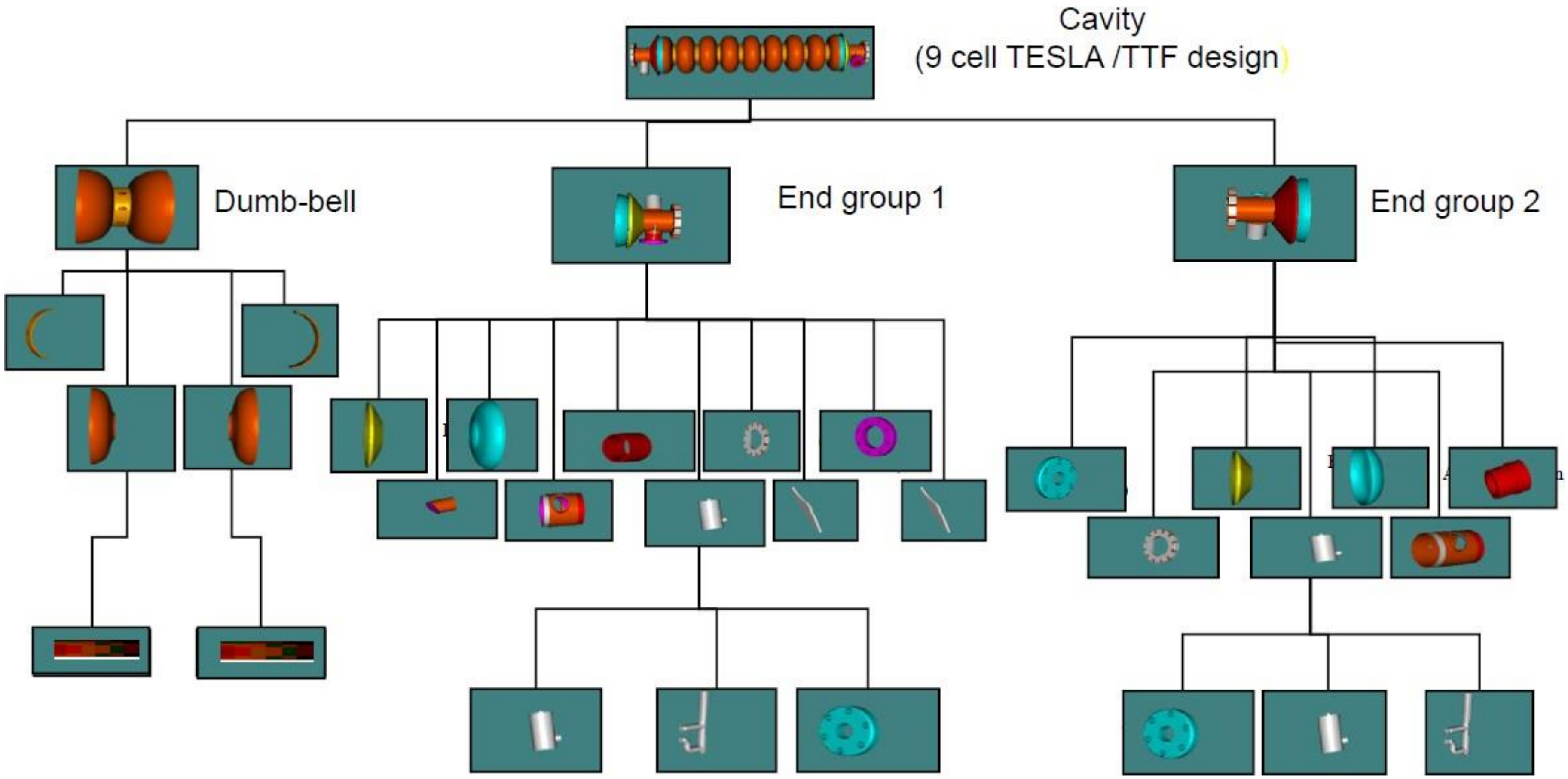

Cavity fabrication: forming half-cells

- The most common fabrication techniques are deep drawing, hydroforming or spinning half-cells.
- Beam pipes and other ports are then fabricated, some parts can be made of a lower grade Nb.
- Alternative techniques (not commonly used): hydroforming and spinning an entire cavity out of single sheet or tube.

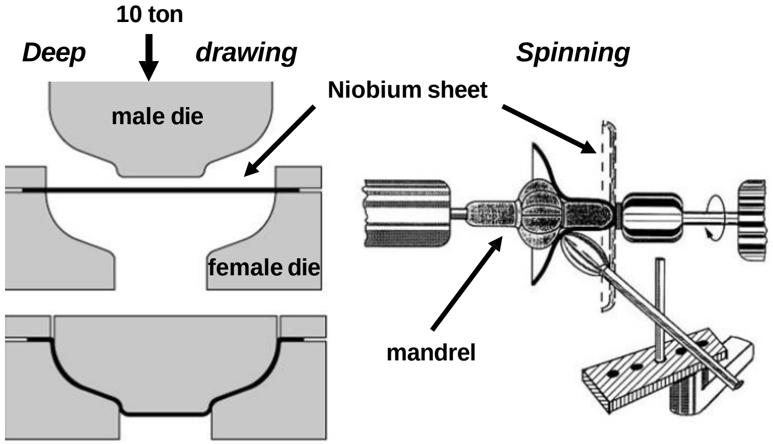

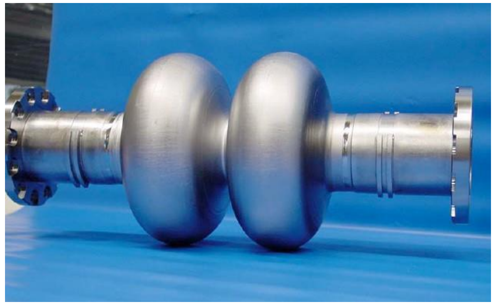

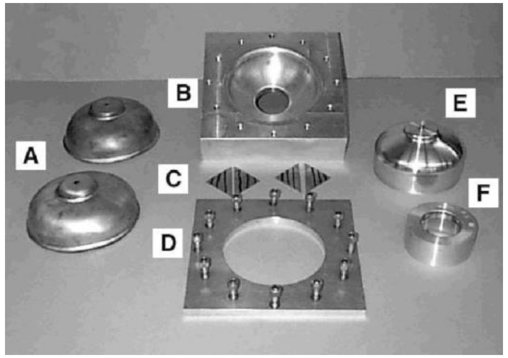

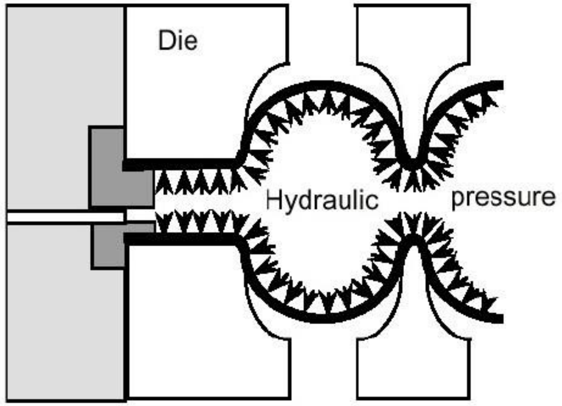

Dumb-bell fabrication steps

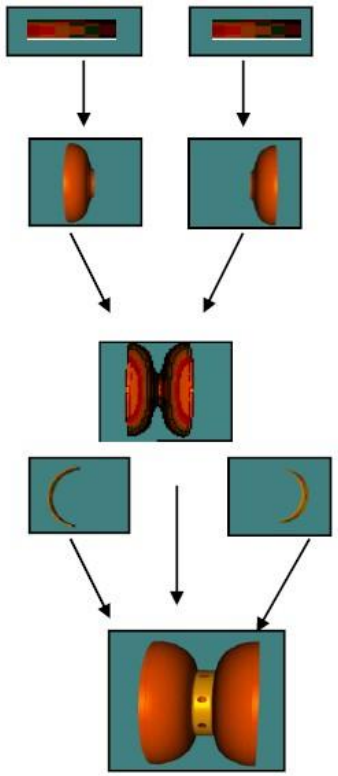

Dumb- bell

1. Mechanical measurement
2. Cleaning (by ultra sonic [us] cleaning +rinsing)
3. Trimming of iris region and reshaping of cups if needed
4. Cleaning
5. Rf measurement of cups
6. Buffered chemical polishing + Rinsing (for welding of Iris)
7. Welding of Iris
8. Welding of stiffening rings
9. Mechanical measurement of dumb-bells
10. Reshaping of dumb bell if needed
11. Cleaning
12. Rf measurement of dumb-bell
13. Trimming of dumb-bells (Equator regions)
14. Cleaning
15. Intermediate chemical etching (BCP /20- 40 μm)+ Rinsing
16. Visual Inspection of the inner surface of the dumb-bell

local grinding if needed + (second chemical treatment + inspection)

Dumb-bell ready for cavity

Electron beam welding

After forming and trim machining, the parts are electron beam welded together.

Welding must be under vacuum, better than 10^{-5} Torr. Things to check:

- Broad welding seam
- Operate with defocused beam
- Smooth underbead
- Overlap at end of welding to avoid accumulation of impurities
- Wait to cool down before opening chamber

Some parts, e.g., flanges, can be brazed to cavity ports.

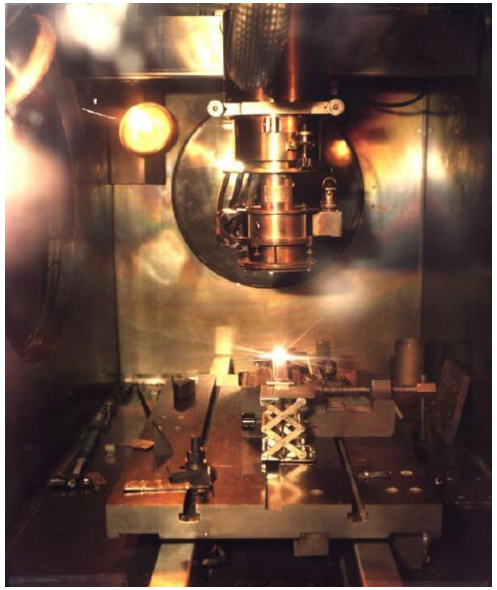

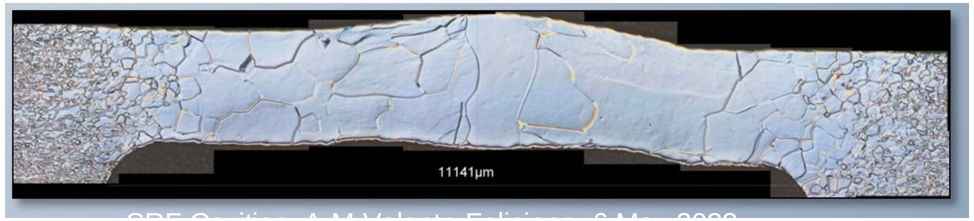

Microstructure of the EB welding area grain size (50 – 2000) µm

Cavity welding steps

Cavity welding: the general way
There are differences of welding processes in industry

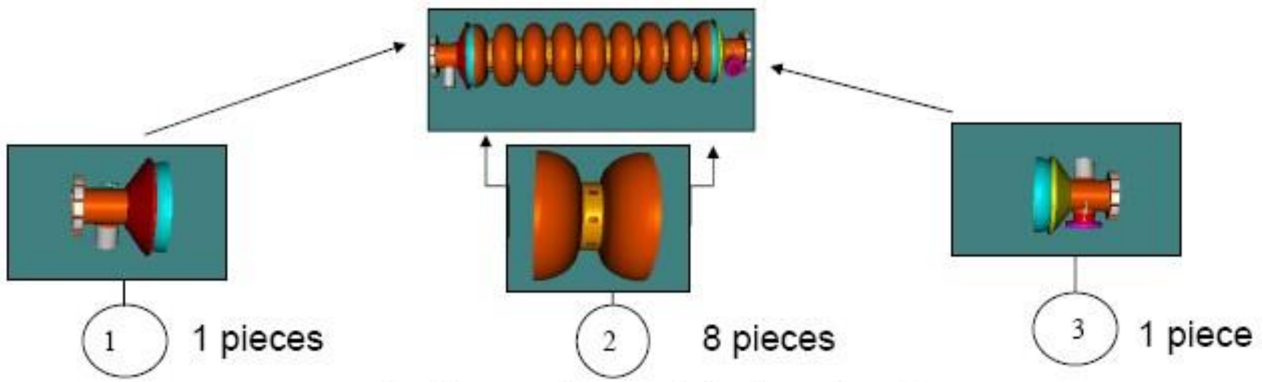

1. Degreasing and rinsing of parts
2. Drying under clean condition
3. Chemical etching at the welding area (Equator)
4. Careful and intensive rinsing with ultra pure water
5. Dry under clean conditions
6. Install parts to fixture under clean conditions
7. Install parts into electron beam (eb) welding chamber (no contamination on the weld area allowed)
8. Install vacuum in the eb welding chamber <= 1E-5 mbar
9. Welding and cool down of Nb to T< 60 C before venting
10. Leak check of weld

Tuning for field flatness

Jefferson Lab

- Cavity frequency and field flatness then checked and tuned. Usually, the goal is to achieve 98% field flatness.
- Set-up for field profile measurements: a metallic needle or bead is perturbing the RF fields while it is pulled through the cavity along its axis. Due to the volume occupied by the bead, the resonance frequency of an eigenmode j is shifted by

$$\left(\frac{f^{(j)\prime}}{f^{(j)}}\right)^2 \approx 1 + \frac{1}{U^{(j)}} \int_{\Delta V_{bead}} \left(\frac{\mu_0}{2}\left|\vec{H}^{(j)}\right|^2 - \frac{\varepsilon_0}{2}\left|\vec{E}^{(j)}\right|^2\right) dv$$

- Since the TM_{010} mode has vanishing magnetic field on axis, we can neglect the first term. Thus, measuring the frequency shift due to the metal bead moving from cell to cell will give us an estimate of the storage energy in each cell.
- Then one proceeds with deforming cells until the desired field flatness is achieved. A couple of iterations with an automated tuning machine is sufficient.

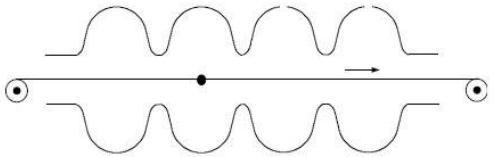

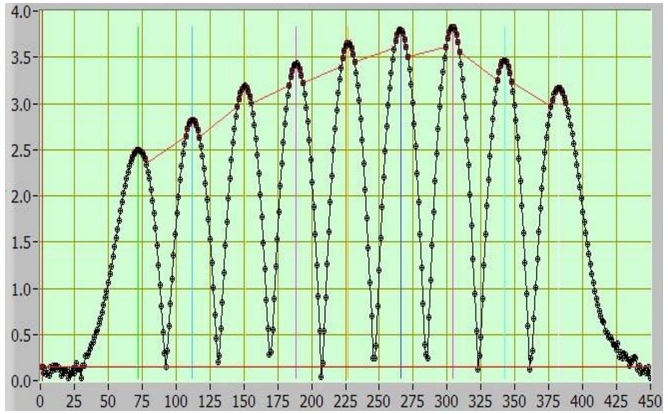

Before tuning. FF 65%, slope +28 %

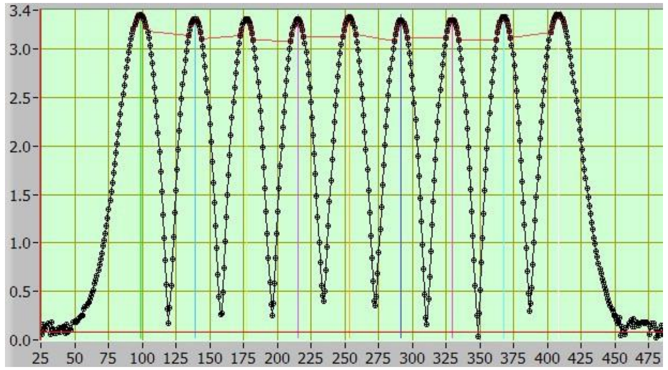

After tuning. FF 98%, slope +0.64 %

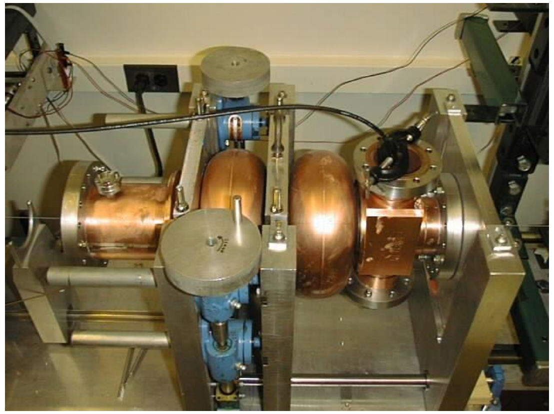

RF measurements

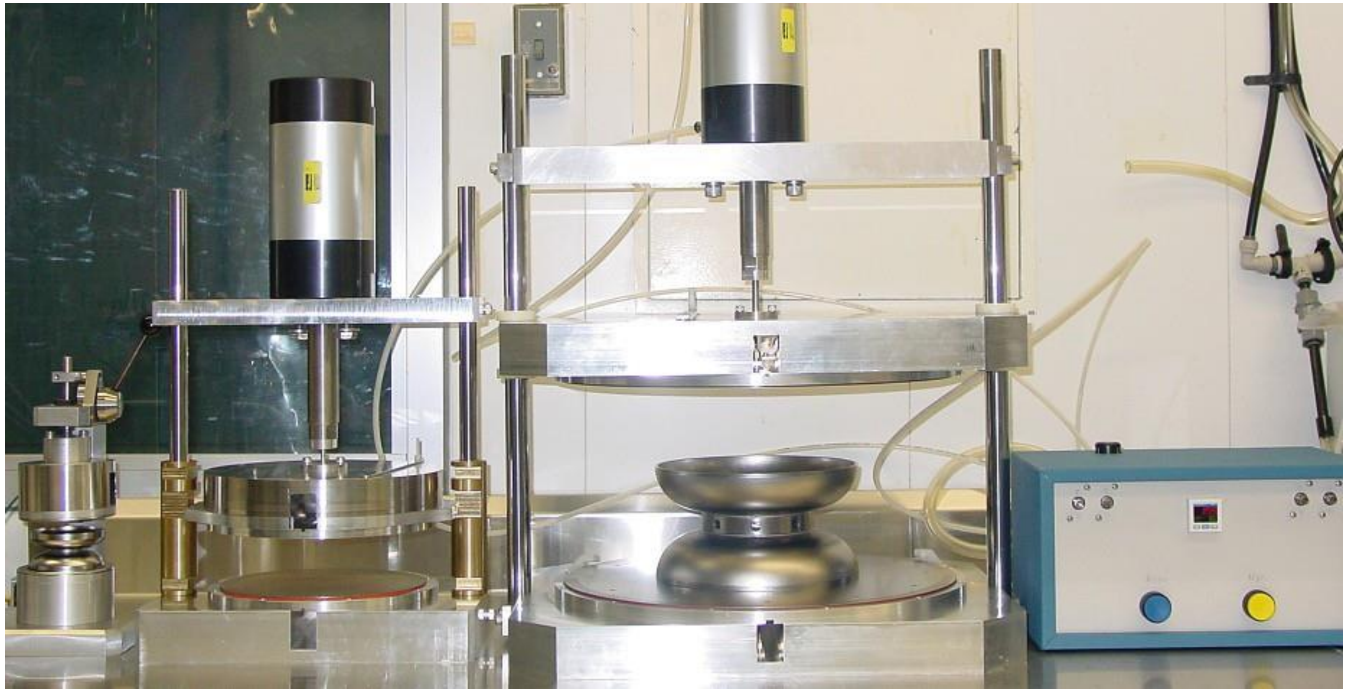

3.9 GHz, 1.3 GHz, 650 MHz dumb-bell measurement fixtures

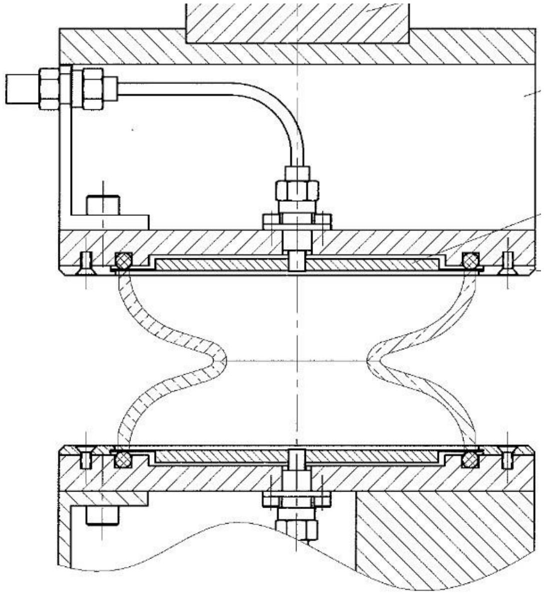

MEASURING OF DUMBELL